

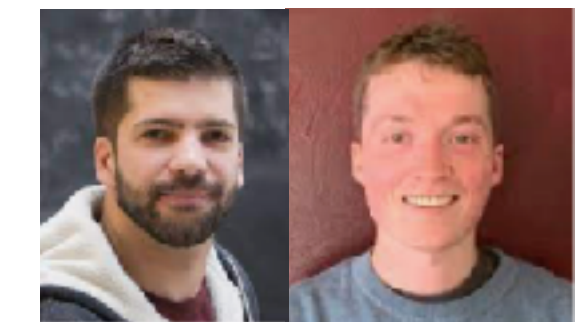
Quantum simulation with Rydberg atom arrays

Roger Melko



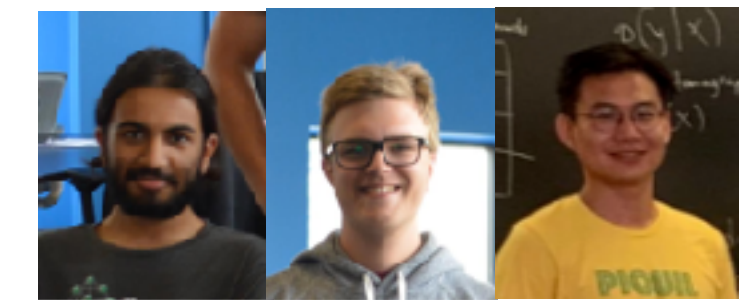
Integrating Neural Networks with a Quantum Simulator for State Reconstruction

G. Torlai, B. Timar, E. van Nieuwenburg, H. Levine, A. Omran, A. Keesling, H. Bernien, M. Greiner, V. Vuletić, M. Lukin, RGM, and M. Endres, Phys. Rev. Lett. 123, 230504 (2019)



Stochastic Series Expansion Quantum Monte Carlo for Rydberg Arrays

E. Merali, I. De Vlucht, RGM, arXiv: 2107.00766 (Scipost)



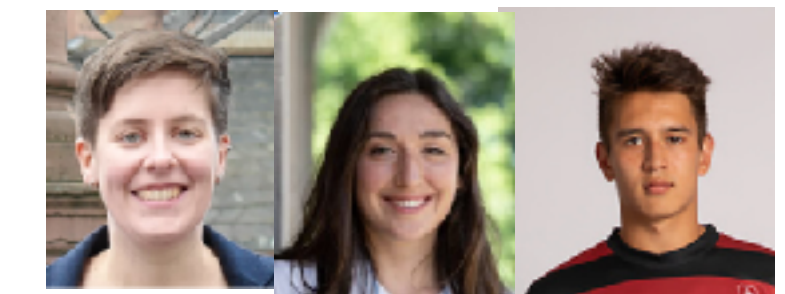
Bulk and Boundary Quantum Phase Transitions in a Square Rydberg Atom Array

M. Kalinowski, R. Samajdar, RGM, M. Lukin, S. Sachdev, S. Choi, arXiv:2112.10790



Enhancing variational Monte Carlo with quantum data

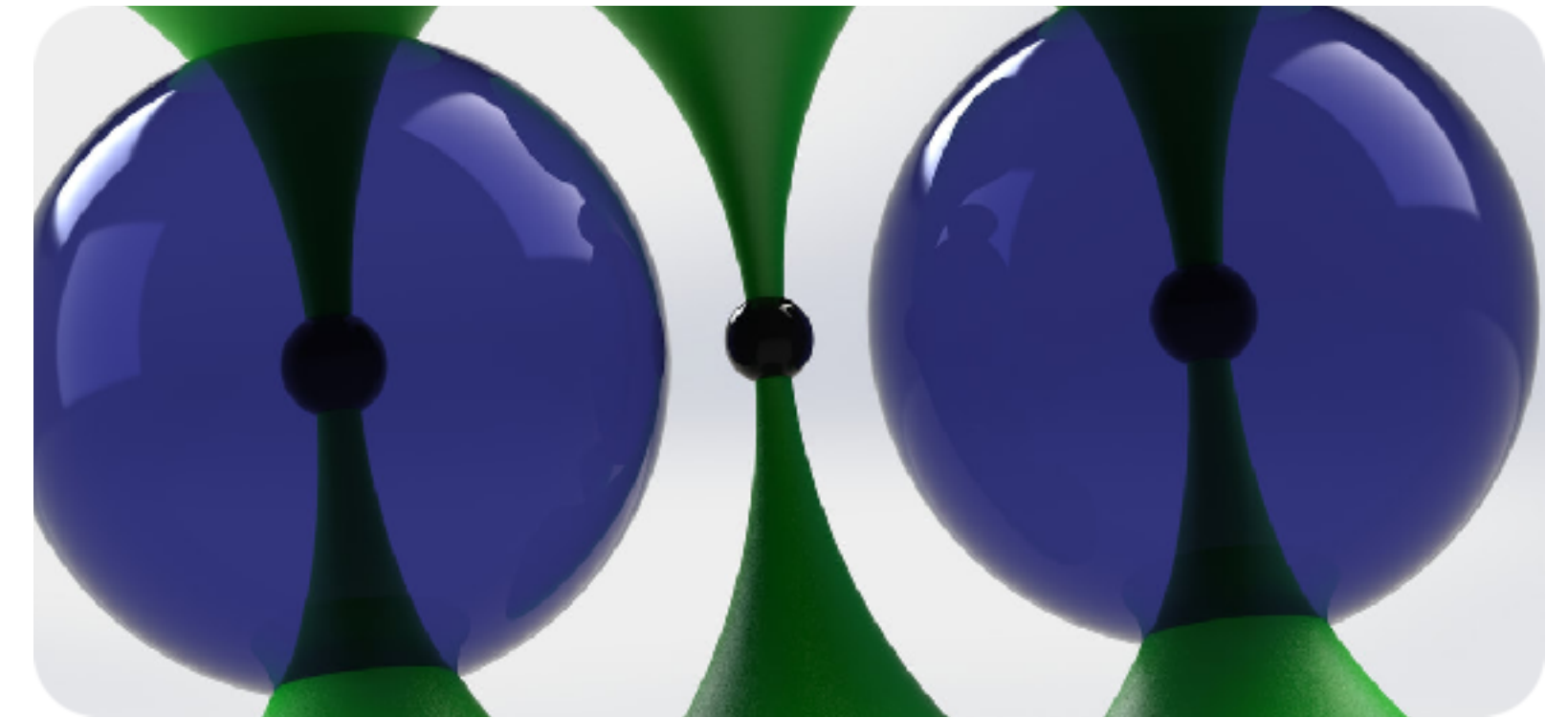
S. Czischek, M. S. Moss, M. Radzihovsky, E. Merali and RGM



Outline

- Rydberg array quantum simulators/emulators
- *In silico* simulation strategies: DMRG, QMC
- Data-driven strategies: neural network wavefunctions & VMC

Rydberg atom arrays



- Neutral atoms (Rb, Sr) are loaded into a lattice formed by an array of optical tweezers
- Atoms can be in their ground state, or an excited state with a large principle quantum number (a Rydberg state). They form a strongly-interacting system.
- Single-atom resolved fluorescent imaging provides projective measurements
- Arrays of atoms are currently used for simulation (groundstates, critical phenomena), solving combinatorial optimization problems

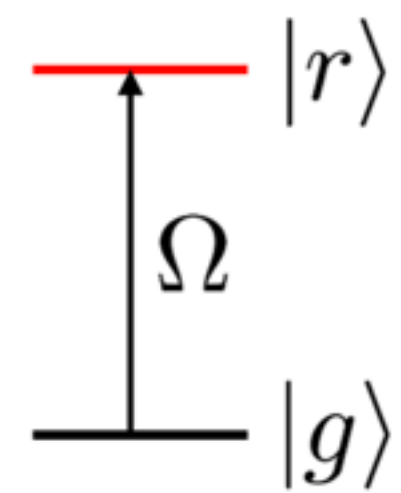


Rydberg Blockade Hamiltonian

Jaksch, Cirac, Zoller, Rolston, Cote, Lukin, Phys. Rev. Lett. 85, 2208 (2000)

Lukin, Fleischhauer, Cote, Duan, Jaksch, Cirac, Zoller, Phys. Rev. Lett. 87, 037901 (2001)

Fendley, Sengupta, Sachdev, Phys. Rev. B 69, 075106 (2004)

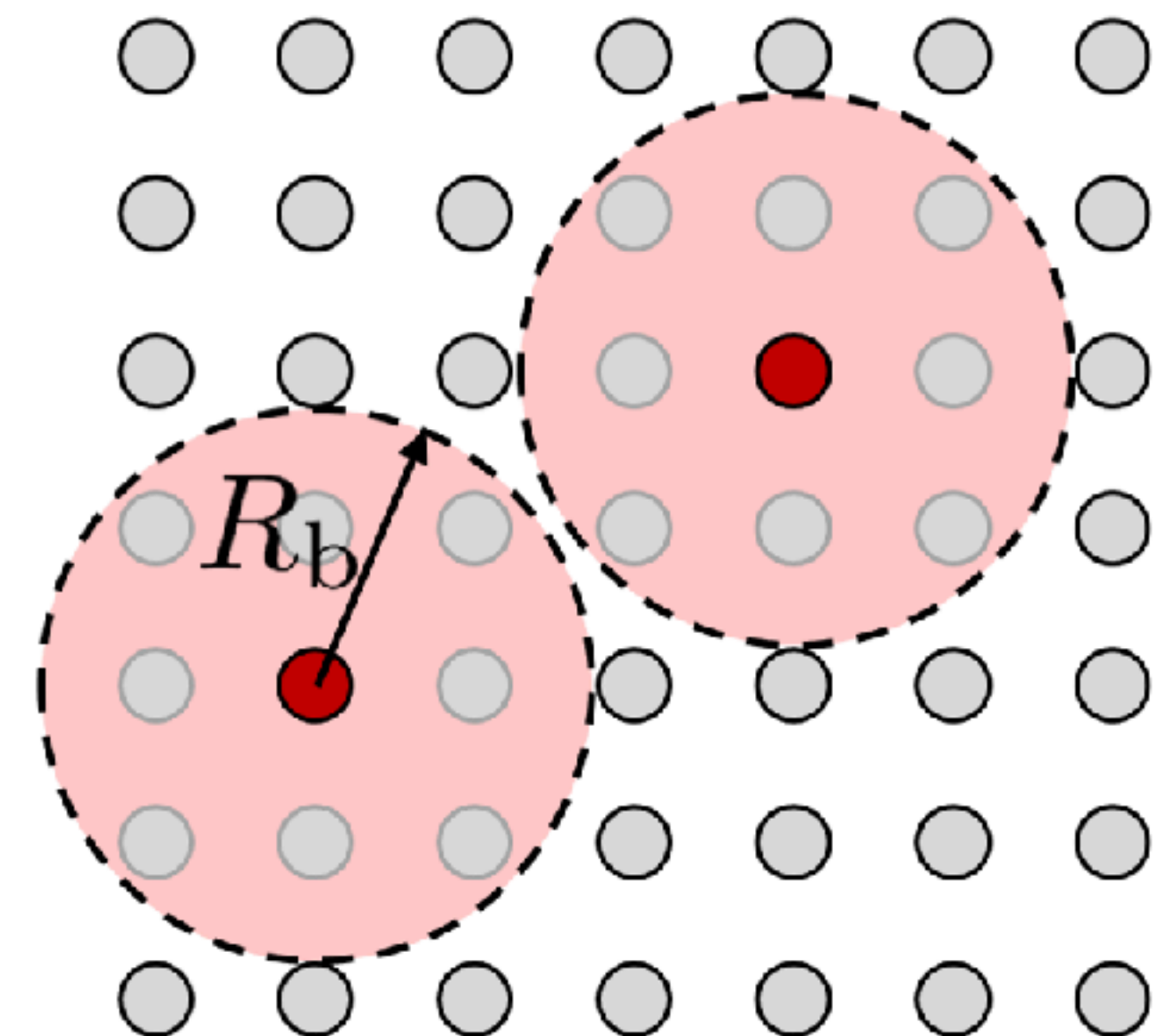


$$H = \Omega \sum_i \sigma_i^x - \Delta \sum_i n_i + \sum_{i < j} V_{ij} n_i n_j$$

$$\sigma^x = |g\rangle\langle r| + |r\rangle\langle g| \quad n = |r\rangle\langle r|$$

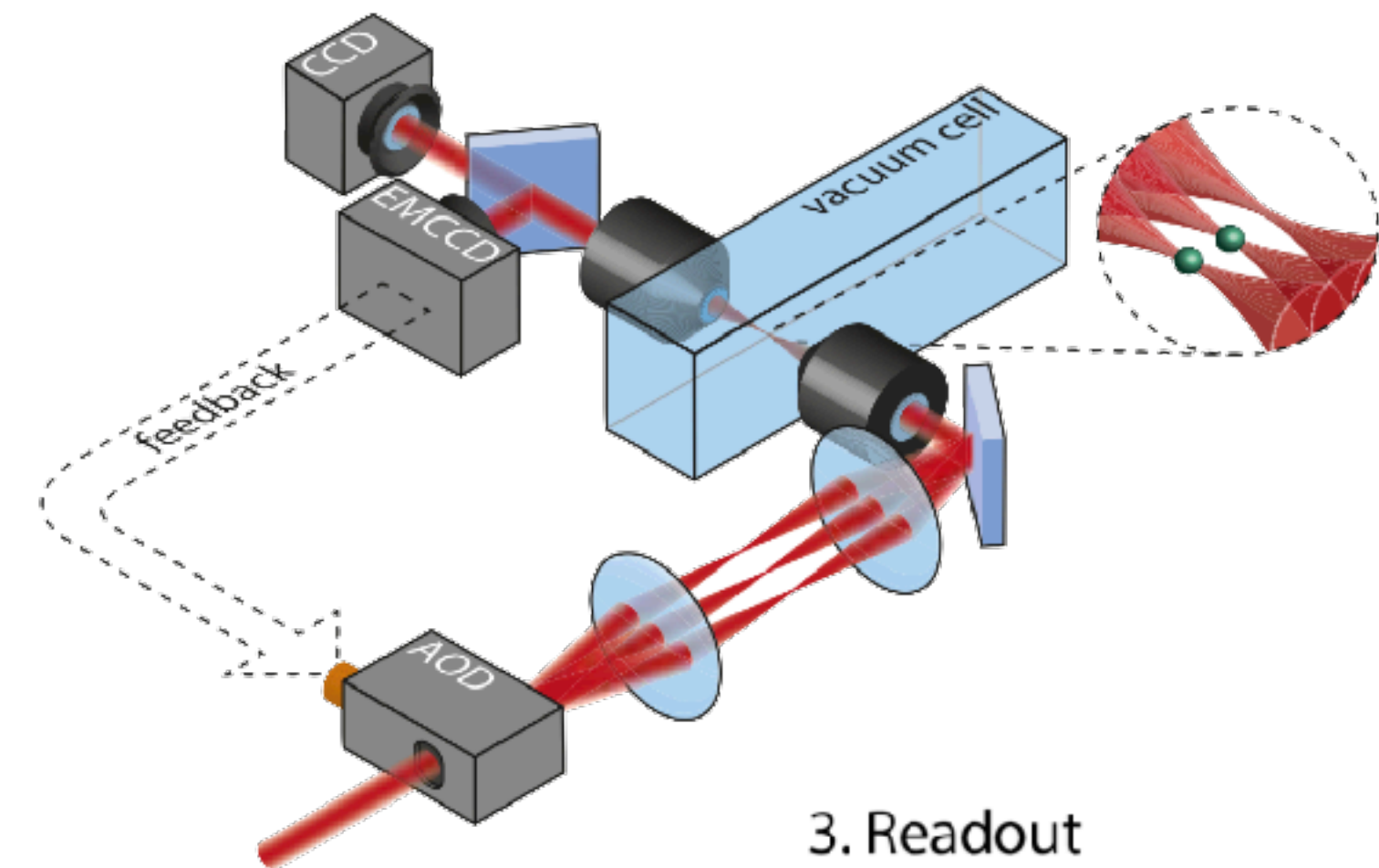
$$V(R) = \frac{\Omega}{(R/R_b)^6}$$

- Two atoms within the blockade radius cannot both be excited into a Rydberg state simultaneously
- Lattice geometry crucially affects physics

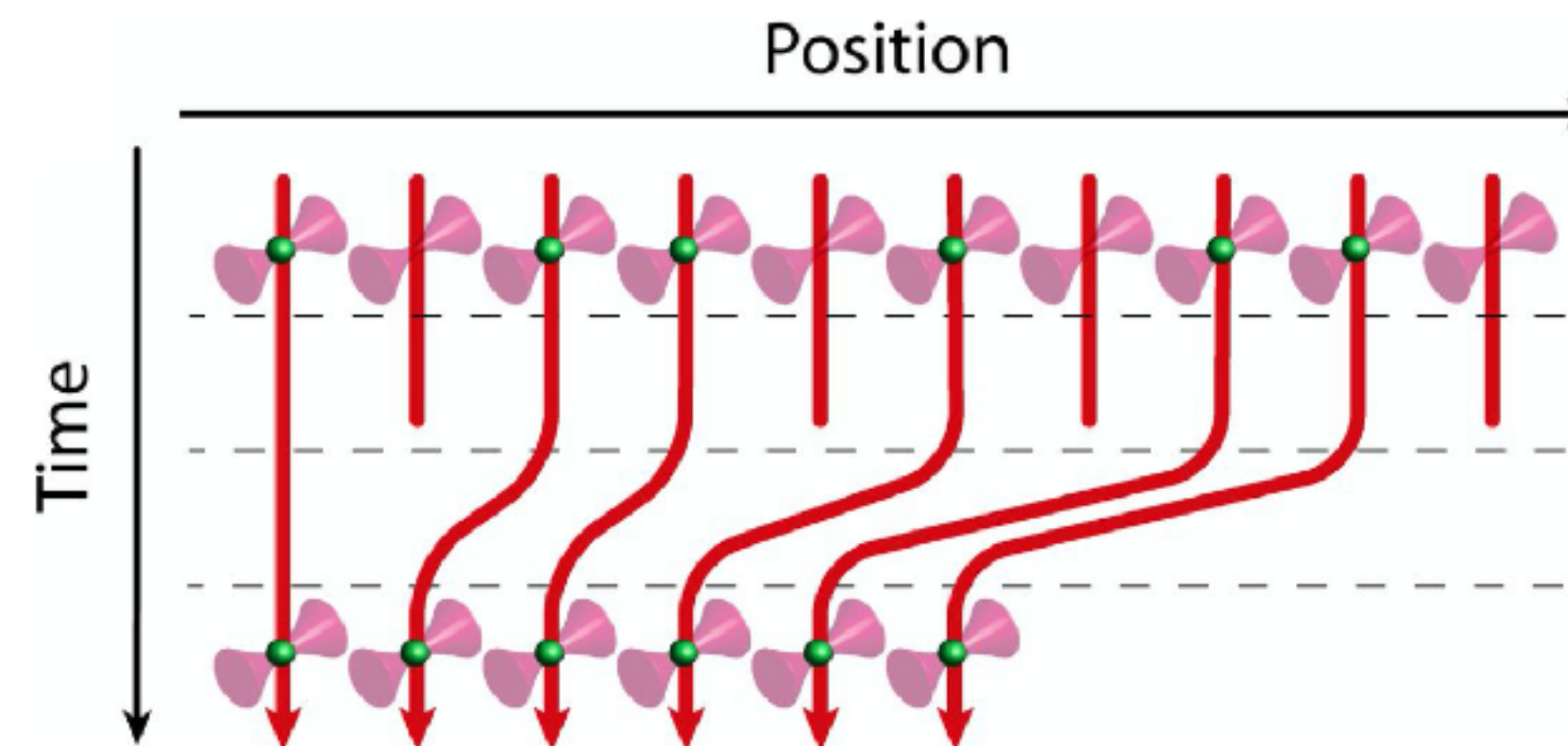
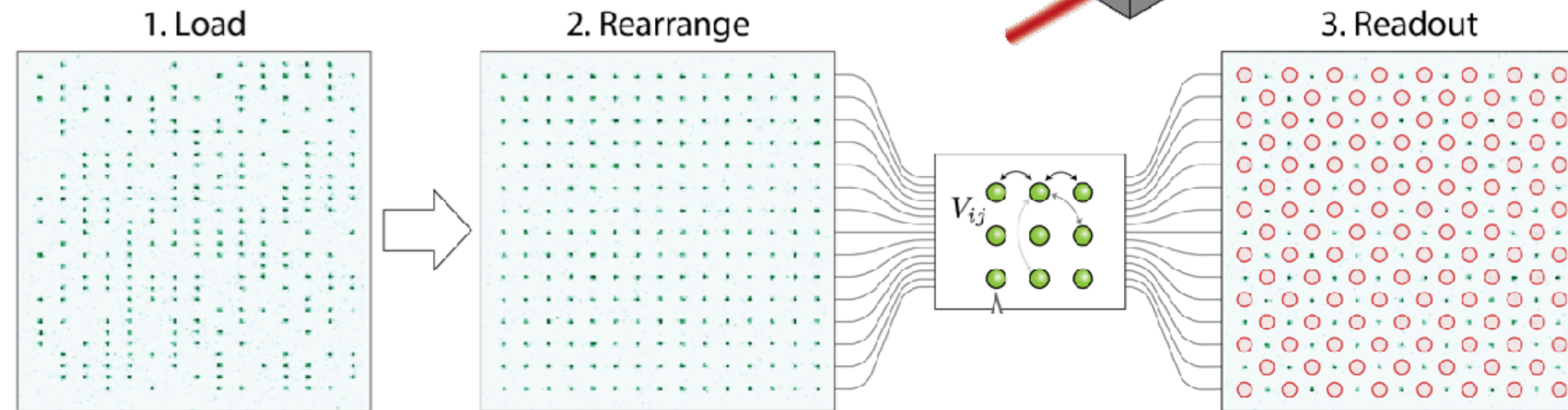
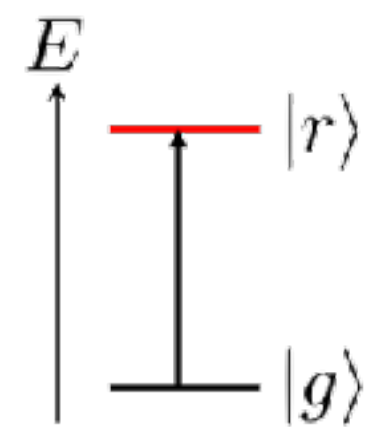


Experimental Rydberg Arrays

Ebadi et. al. arXiv:2012.12281
Nature 595, 227 (2021)



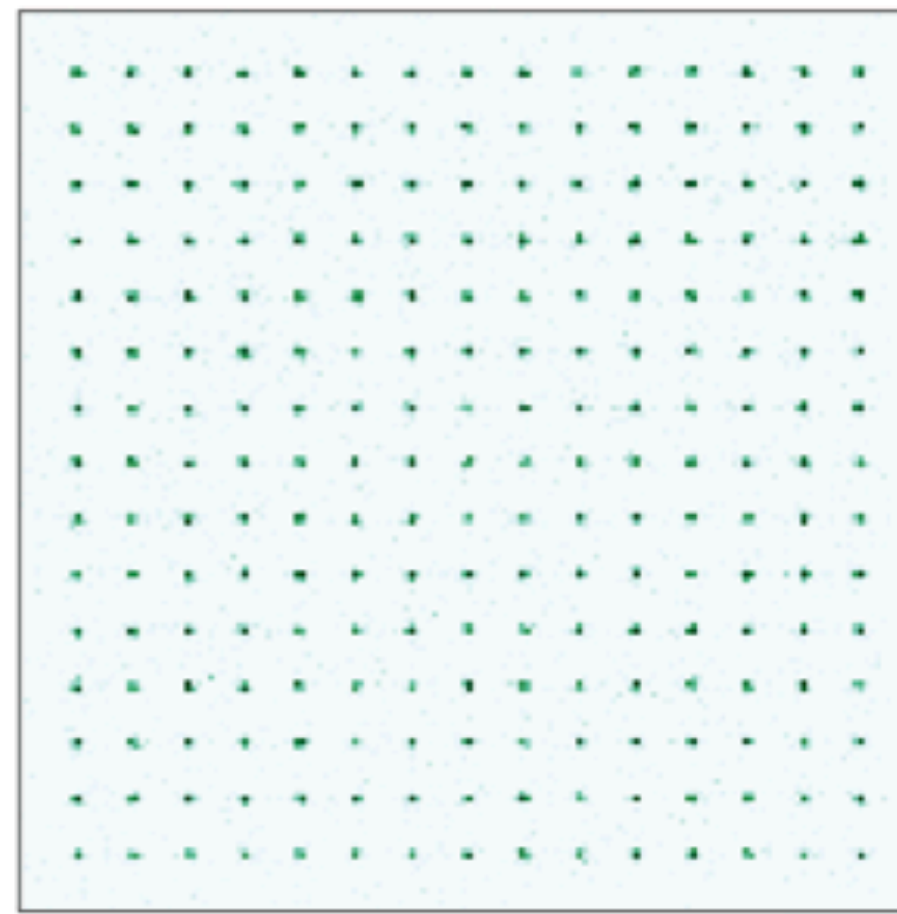
^{87}Rb



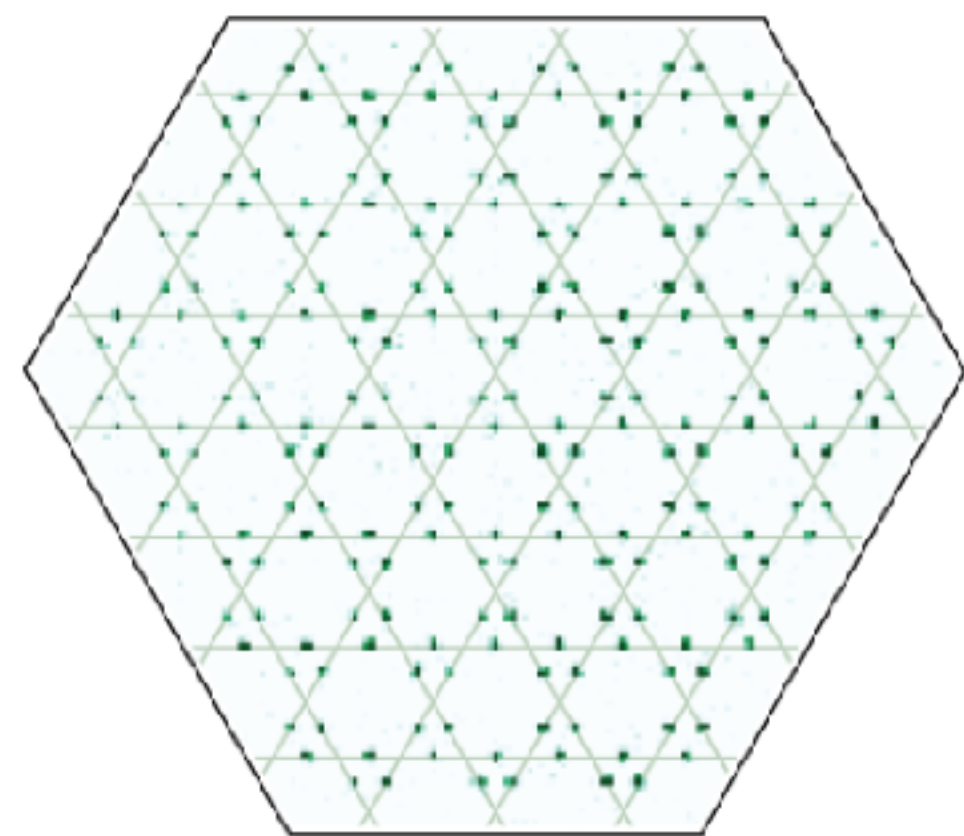
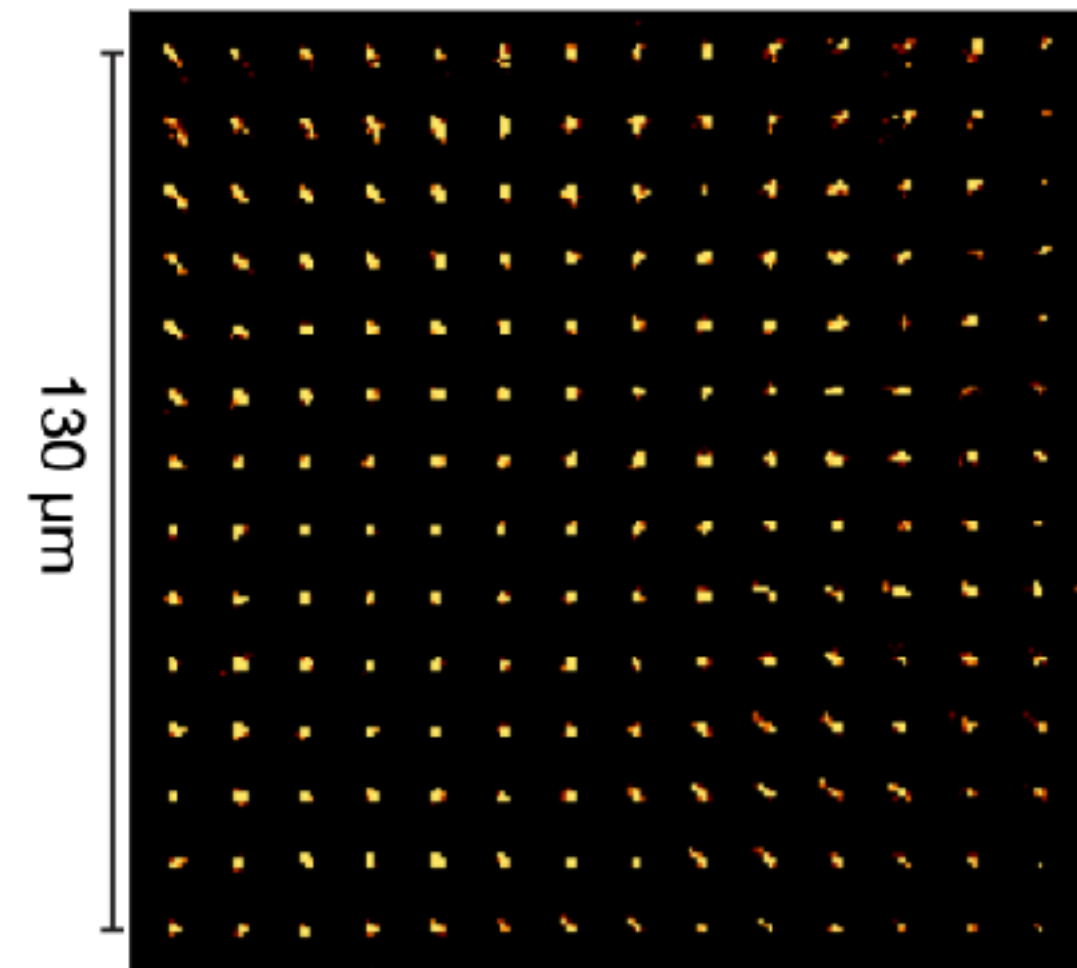
Single-atom resolved fluorescent imaging provides projective measurements of $|g\rangle$

Endres et. al. Science 354, 1024 (2016)

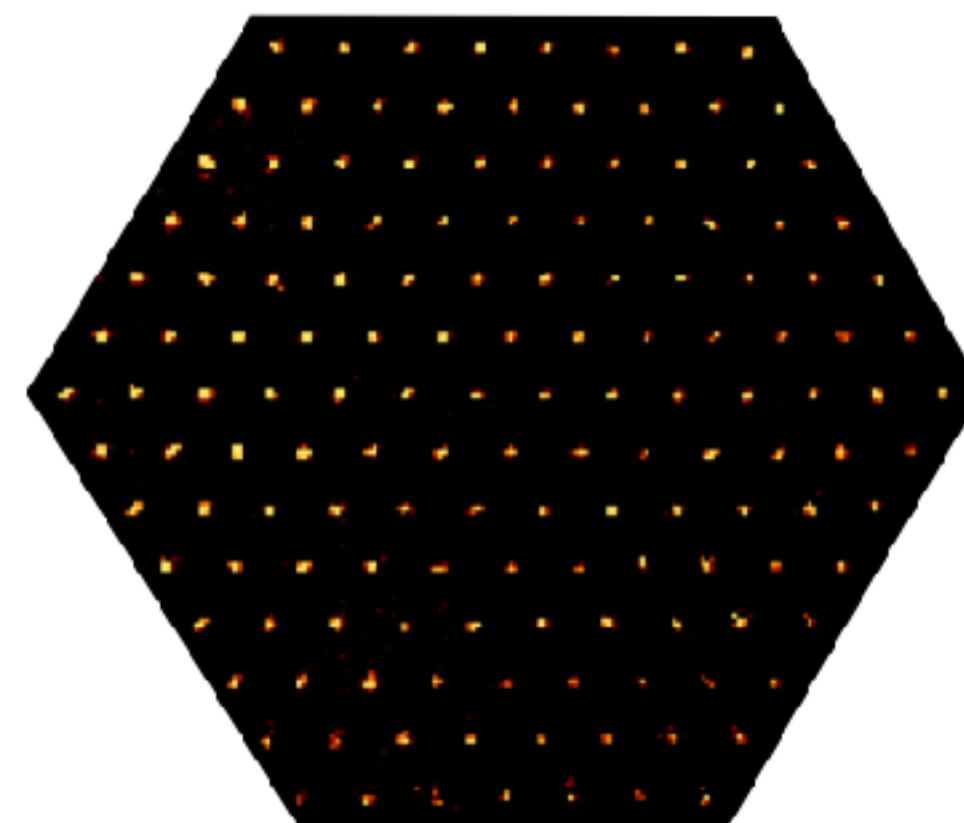
Experimental lattices



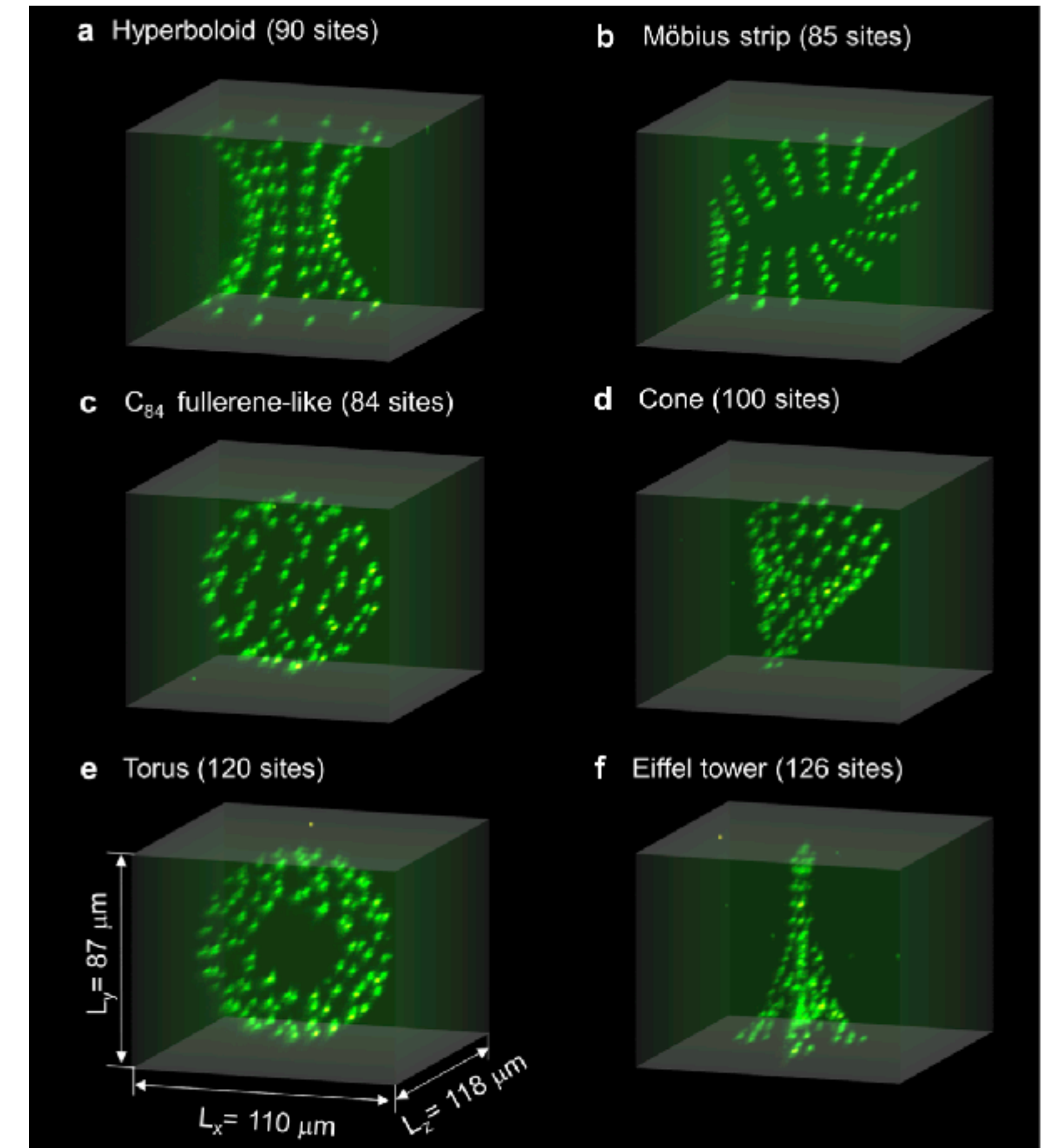
Ebadi et. al. arXiv:2012.12281
Nature 595, 227 (2021)



Semeghini et. al. arXiv:2104.04119
Science, 374, 1242 (2021)



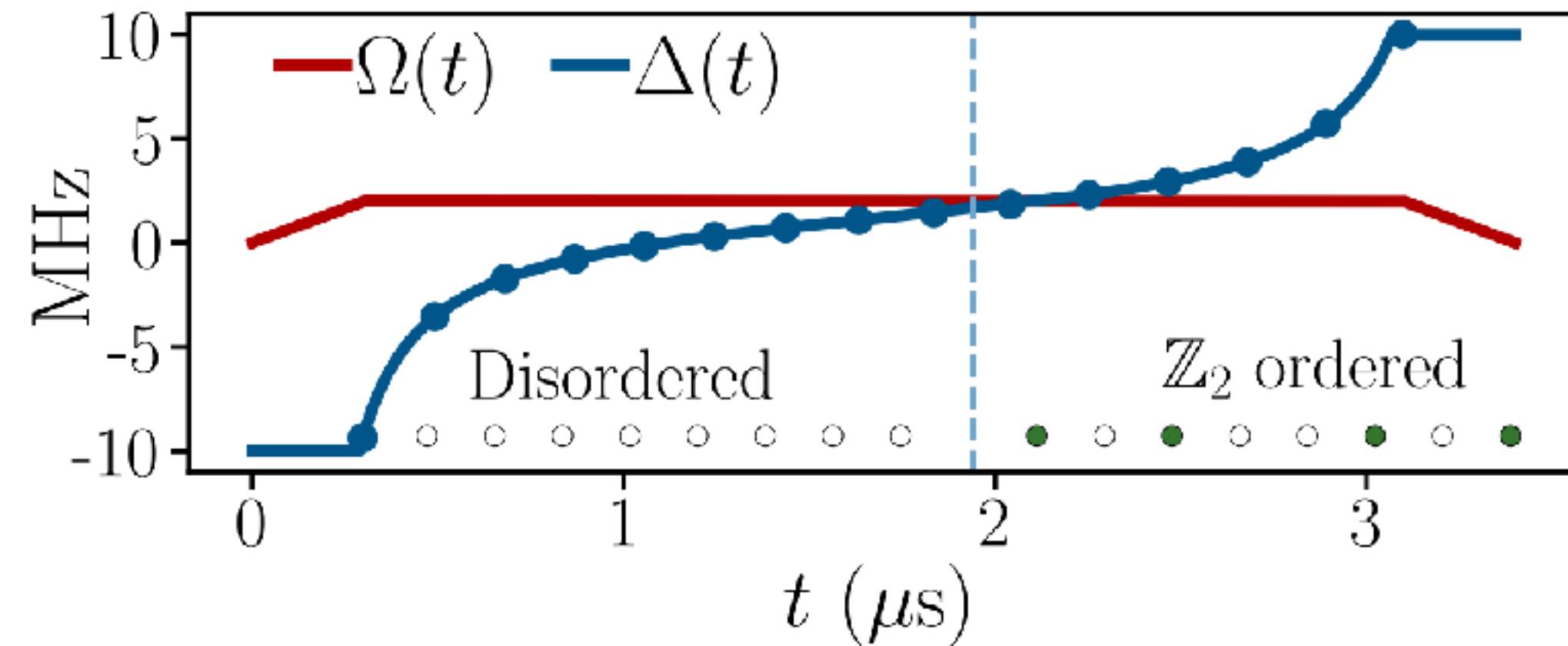
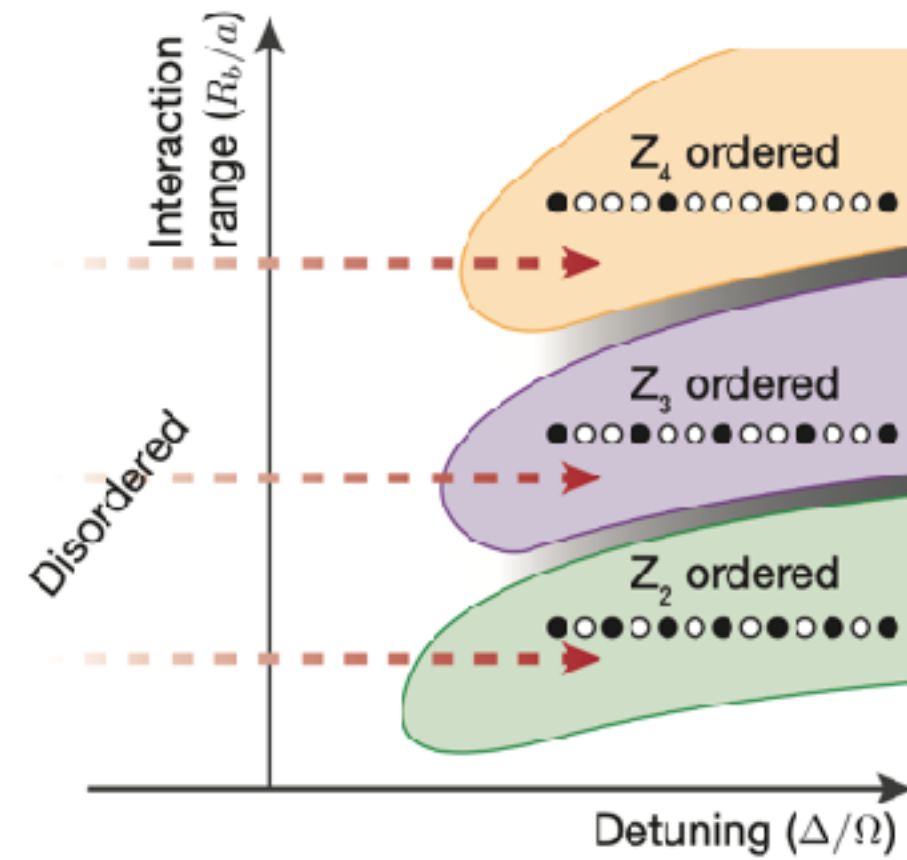
Scholl et al. arXiv:2012.12268
Nature 595, 233 (2021)



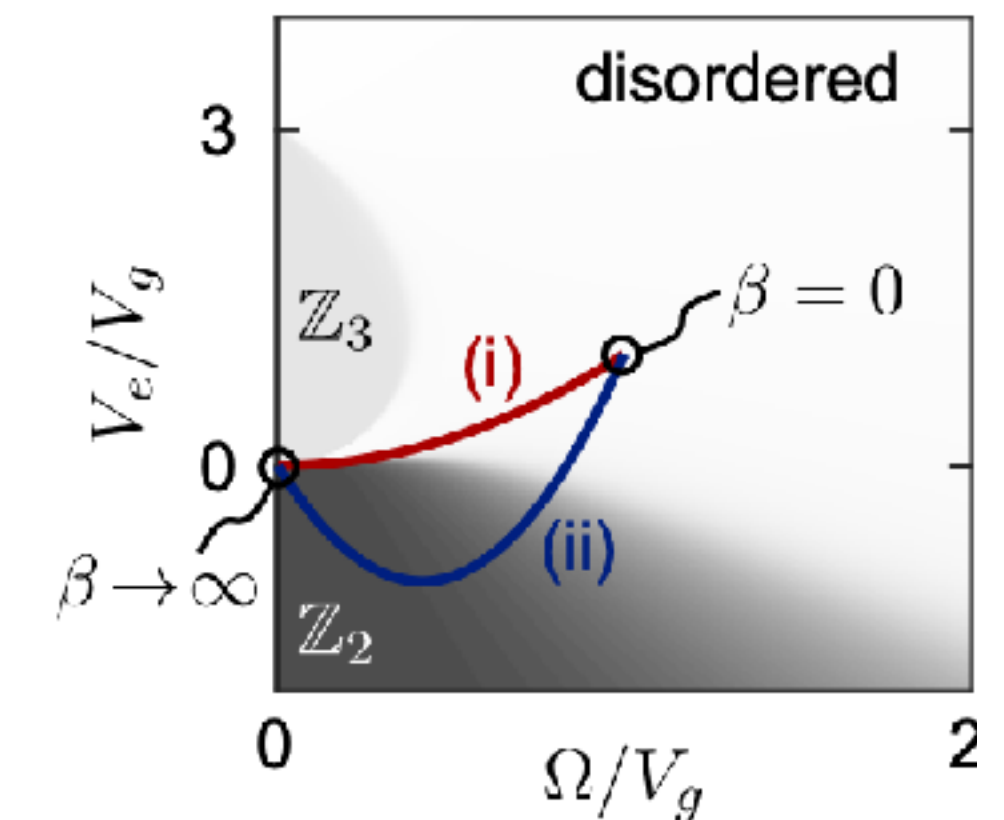
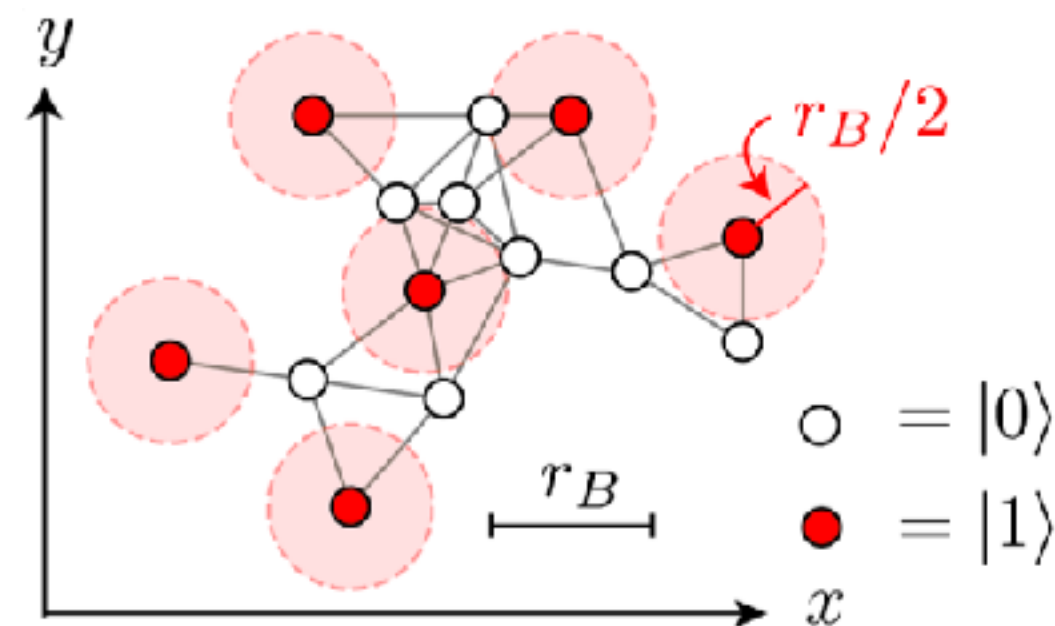
Barredo, Lienhard, de Léséleuc, Lahaye, Browaeys
Nature 561, (2018)

Adiabatic state preparation

- Phase diagrams are studied by detuning across the bare resonance



- Optimization problems (MIS) and quantum sampling

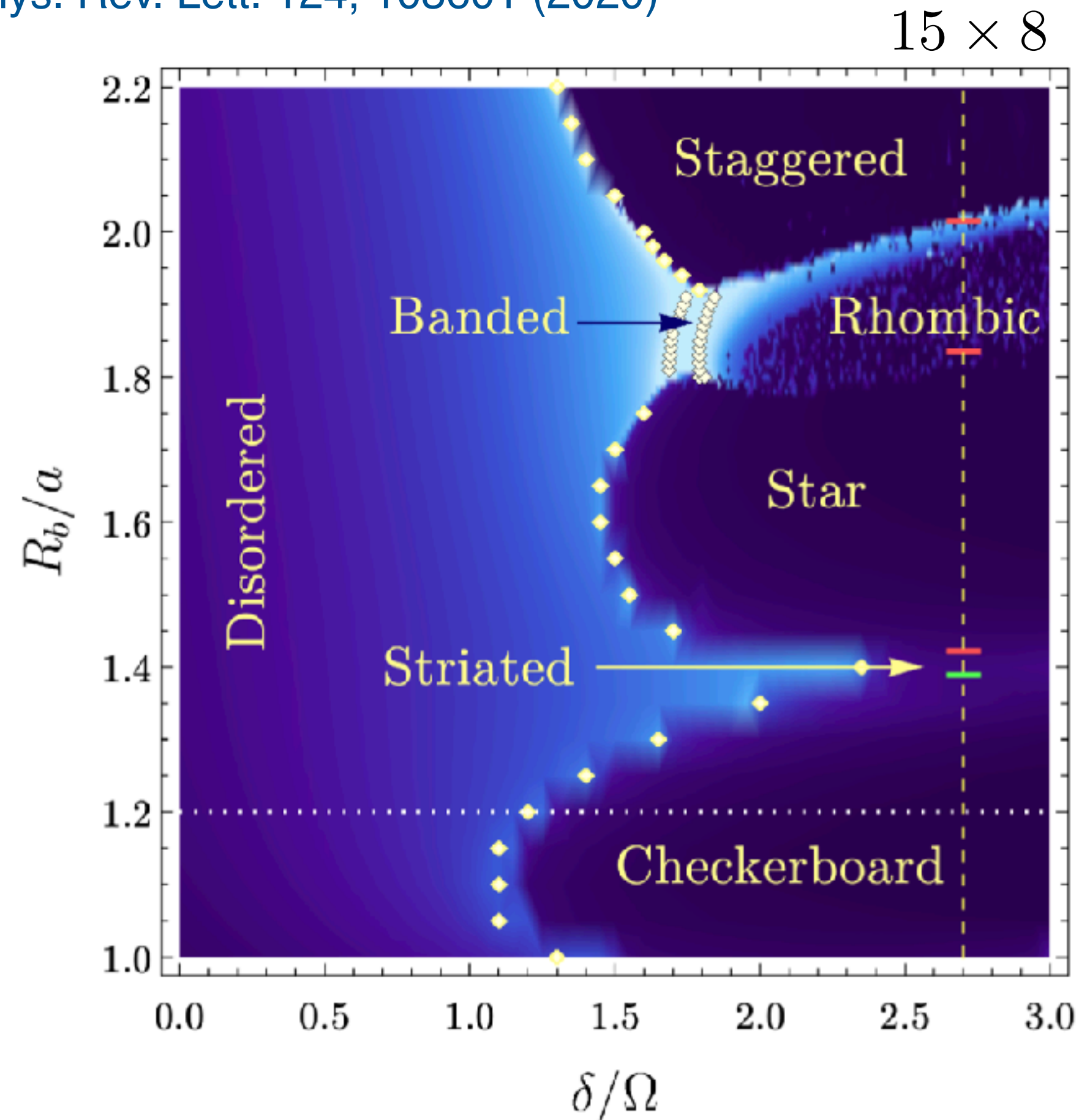


H. Pichler, S.-T. Wang, L. Zhou, S. Choi, and M. D. Lukin,
 Quantum optimization for maximum independent set using Rydberg atom arrays, arXiv:1808.10816,
 Computational complexity of the Rydberg blockade in two dimensions, arXiv:1809.04954

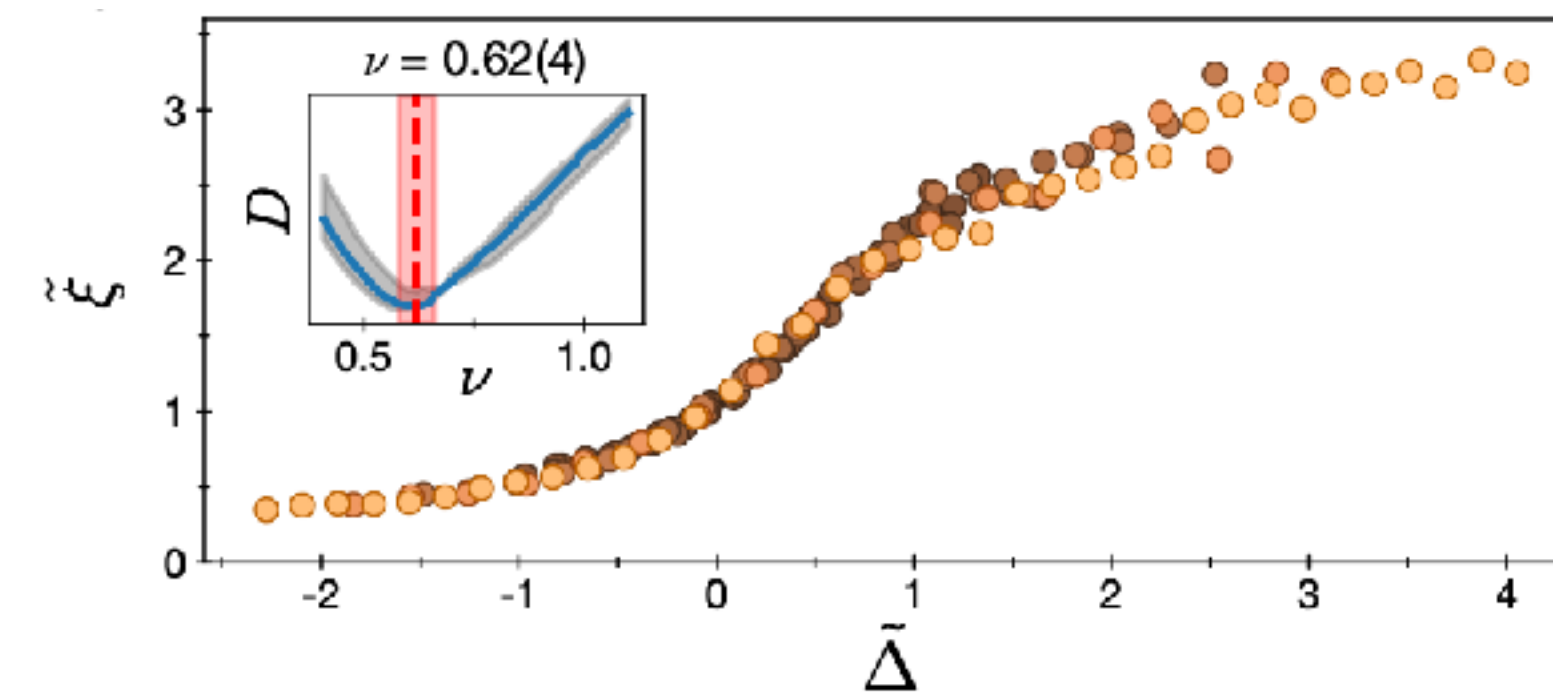
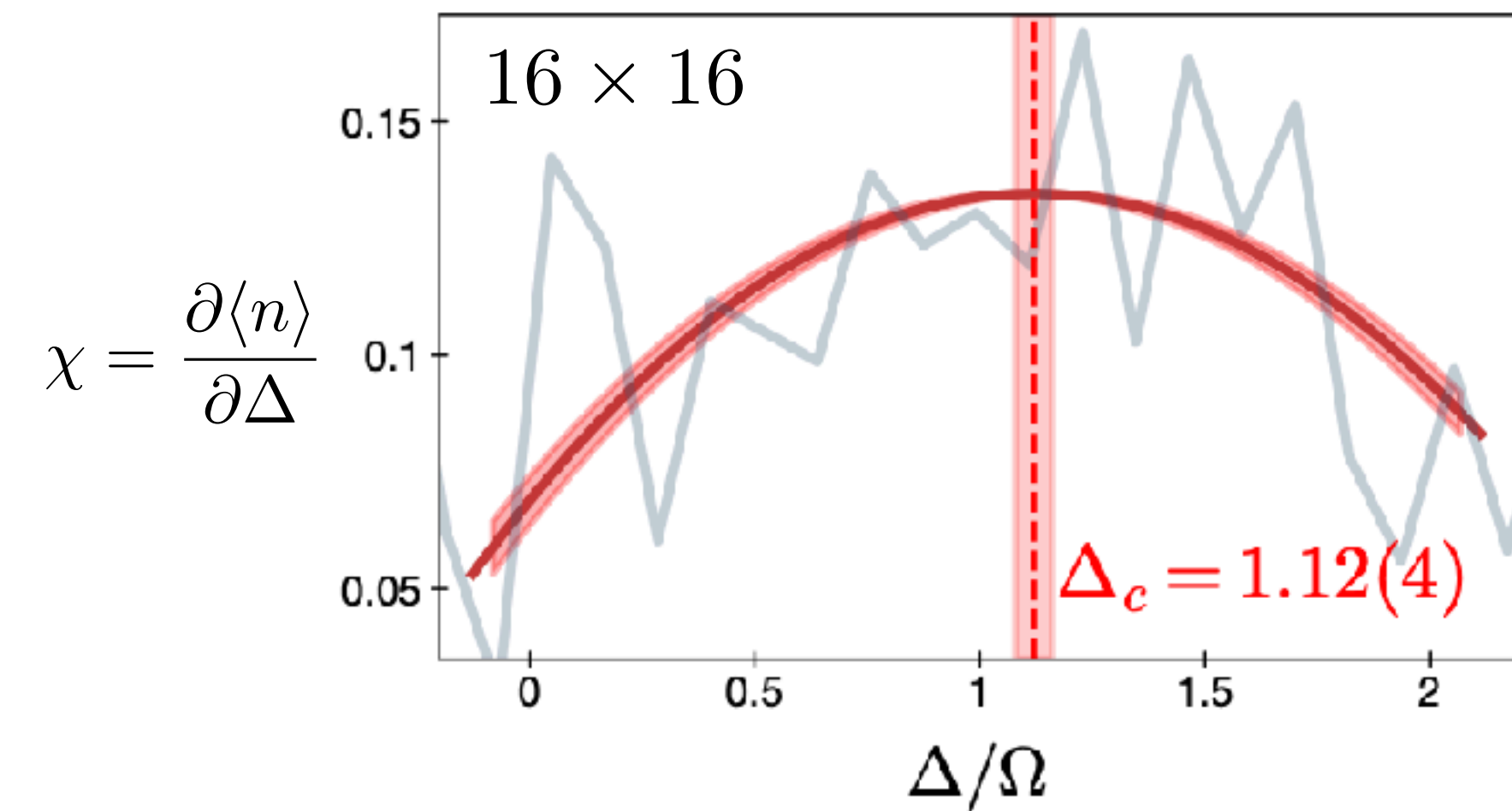
D. Wild, D. Sels, H. Pichler, C. Zanoci, M. Lukin
 Quantum Sampling Algorithms for Near-Term Devices
 arXiv:2005.14059, arXiv:2109.03007

2D: Quantum critical points

Samajdar, Ho, Pichler, Lukin, Sachdev,
Phys. Rev. Lett. 124, 103601 (2020)



Ebadi et. al. arXiv:2012.12281
Nature 595, 227 (2021)



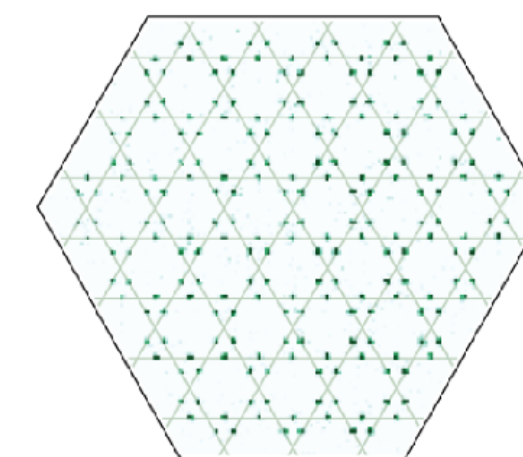
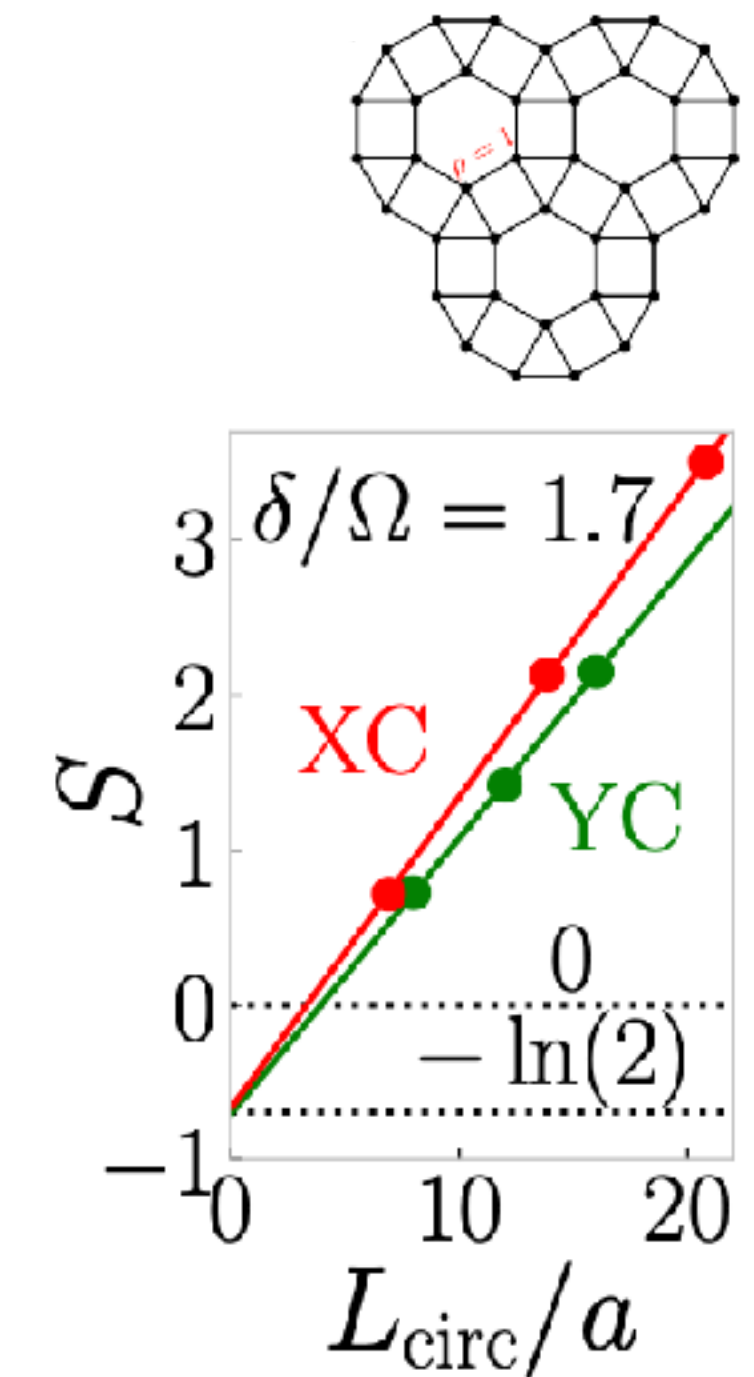
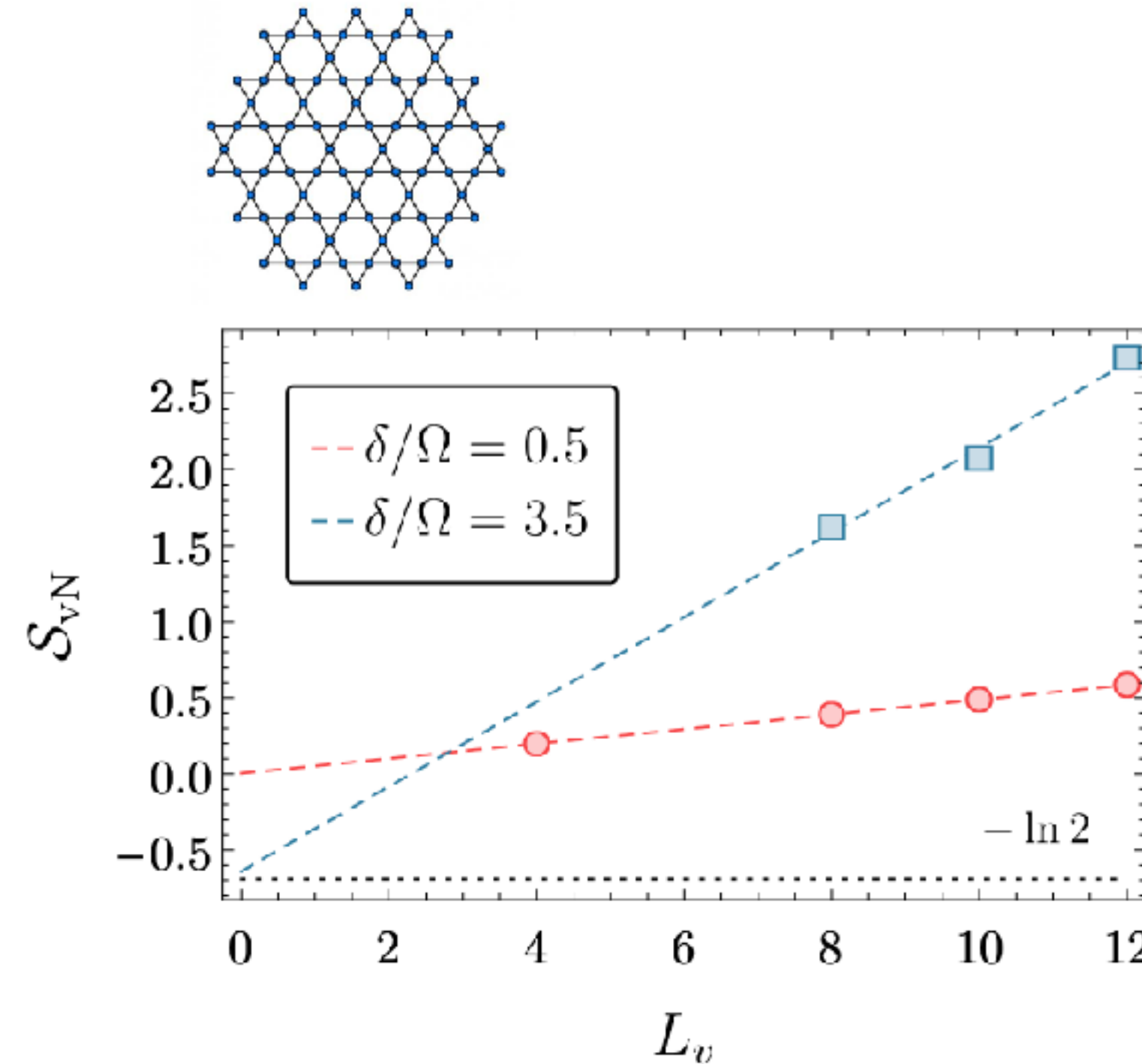
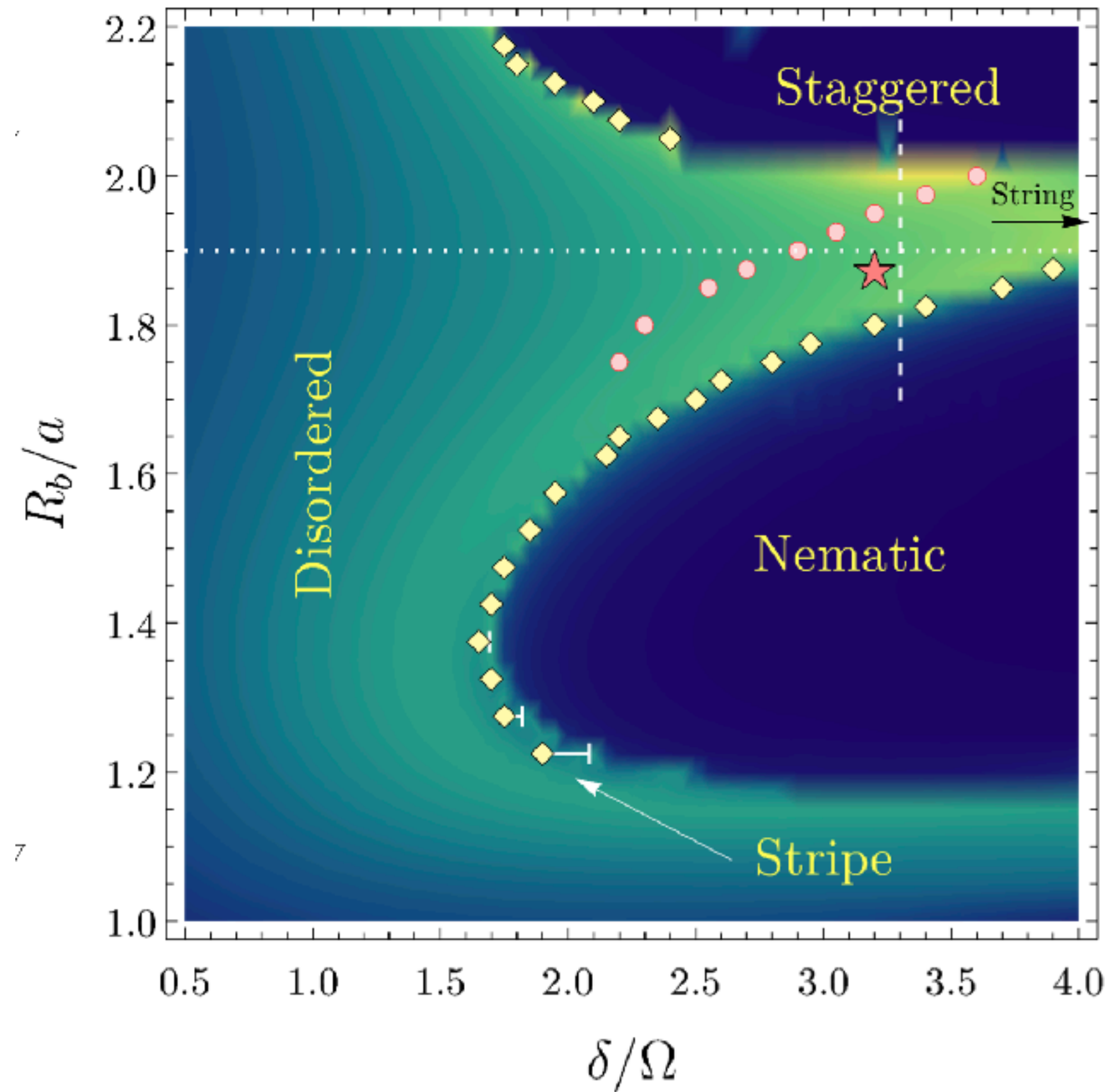
- First experimental realization of a 2+1 D QCP in the Ising universality class

2D: Quantum spin liquids

Samajdar, Ho, Pichler, Lukin, Sachdev, Proc. Natl. Acad. Sci. 118 (2021)
 Verresen, Lukin, Vishwanath, Phys. Rev. X 11, 031005 (2021)

$$S = aL - \ln(2)$$

Signature of a Z2 spin liquid S_{topo}



Semeghini et. al. arXiv:2104.04119
 (219 atoms)

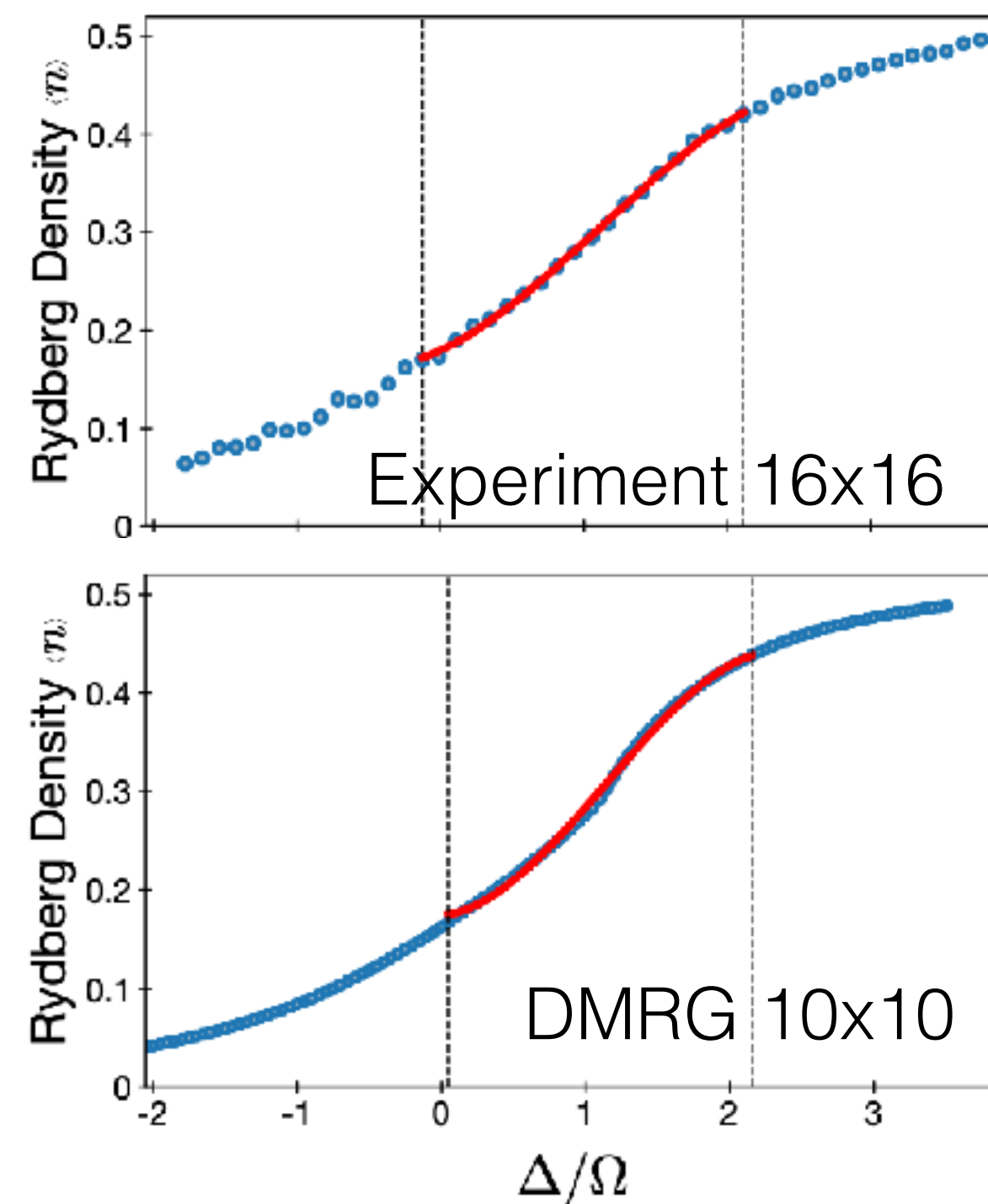
- Motivating experimental searches

Outline


- Rydberg array quantum simulators/emulators
- *In silico* simulation strategies: DMRG, QMC
- Data-driven strategies: neural network wavefunctions & VMC

in silico simulation strategies: **DMRG/MPS**

Ebadi et. al. Nature 595, 227 (2021)



Quantum simulation of 2D antiferromagnets with hundreds of Rydberg atoms

Pascal Scholl , Michael Schuler, Hannah J. Williams, Alexander A. Eberharter, Daniel Barredo, Kai-Niklas Schymik, Vincent Lienhard, Louis-Paul Henry, Thomas C. Lang, Thierry Lahaye, Andreas M. Läuchli & Antoine Browaeys

Nature **595**, 233–238 (2021)

“MPS simulations for systems up to $L = 10$ are reliable to characterize and benchmark the experimental results, although they might not be fully converged in χ with regard to other observables, such as the entanglement entropy. Finally, we want to mention that reliable simulations of the dynamics for the largest experimental results achieved in this paper ($L = 14$) seem to be out of reach with currently available computational hardware...”

- DMRG/MPS is currently the standard for comparison with experiment
- Enabled by open source libraries such as iTensor and TeNPy

in silico simulation strategies: QMC

Note: the Rydberg Hamiltonian is (efficiently made) stoquastic

$$H = \Omega \sum_i \sigma_i^x - \Delta \sum_i n_i + \sum_{i < j} V_{ij} n_i n_j$$
$$H = \begin{pmatrix} d & -|o\rangle & -|o\rangle & -|o\rangle & -|o\rangle \\ -|o\rangle & d & -|o\rangle & -|o\rangle & -|o\rangle \\ -|o\rangle & -|o\rangle & d & -|o\rangle & -|o\rangle \\ -|o\rangle & -|o\rangle & -|o\rangle & d & -|o\rangle \\ -|o\rangle & -|o\rangle & -|o\rangle & -|o\rangle & d \end{pmatrix}$$

- Allows for (efficient?) simulation by quantum Monte Carlo

$$Z = \text{Tr} \left\{ e^{-\beta \hat{H}} \right\} = \sum_{\alpha_0} \langle \alpha_0 | \sum_{n=0}^{\infty} \frac{\beta^n}{n!} (-\hat{H})^n | \alpha_0 \rangle$$
$$Z \equiv \langle \psi_0 | \psi_0 \rangle = \langle \alpha_\ell | (-\hat{H})^M (-\hat{H})^M | \alpha_r \rangle$$

- Perron-Frobenius guarantees a real/positive groundstate wavefunction

$$\psi_\lambda(\mathbf{x}) = \sqrt{p_\lambda(\mathbf{x})}$$

Efficient QMC: sign-free and ergodic

Stochastic series expansion

$$\hat{H} = \frac{\Omega}{2} \sum_{i=1}^N \hat{\sigma}_i^x - \delta \sum_{i=1}^N \hat{n}_i + \sum_{i<j} V_{ij} \hat{n}_i \hat{n}_j$$

Sandvik, Phys. Rev. E 68(5), 056701 (2003)
 Merali, De Vlugt, RGM, arXiv:2107.00766
 (c.f. Kalinowski *et al.* arXiv:2112.10790)

$$\langle 1 | \hat{H}_{-1,a} | 0 \rangle = \langle 0 | \hat{H}_{-1,a} | 1 \rangle = \frac{\Omega}{2},$$

$$\langle 1 | \hat{H}_{1,a} | 1 \rangle = \langle 0 | \hat{H}_{1,a} | 0 \rangle = \frac{\Omega}{2},$$

$$W_{ij}^{(1)} \equiv \langle 00 | \hat{H}_{1,b} | 00 \rangle = C_{ij},$$

$$W_{ij}^{(2)} \equiv \langle 01 | \hat{H}_{1,b} | 01 \rangle = \delta_b + C_{ij},$$

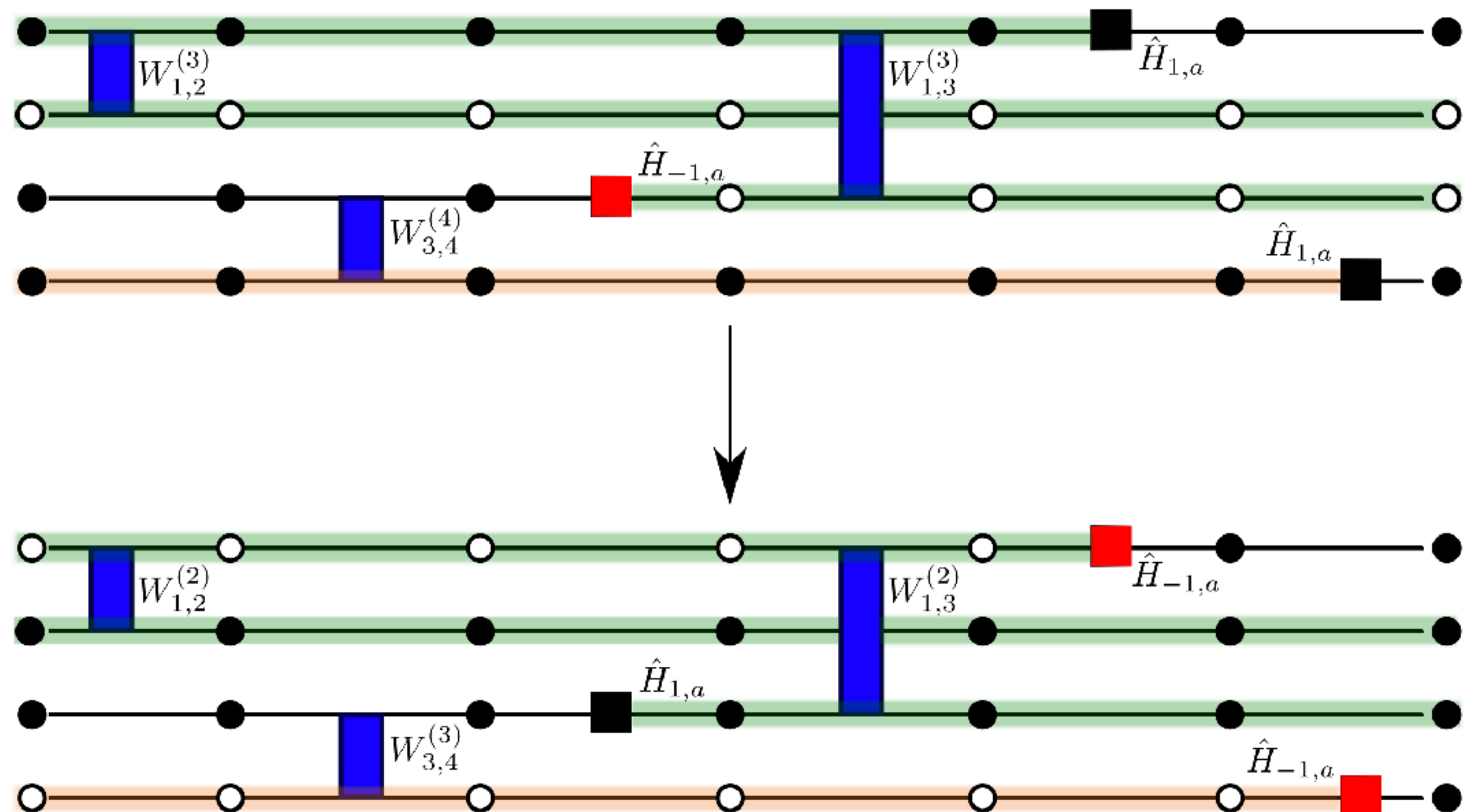
$$W_{ij}^{(3)} \equiv \langle 10 | \hat{H}_{1,b} | 10 \rangle = \delta_b + C_{ij},$$

$$W_{ij}^{(4)} \equiv \langle 11 | \hat{H}_{1,b} | 11 \rangle = -V_{ij} + 2\delta_b + C_{ij}$$

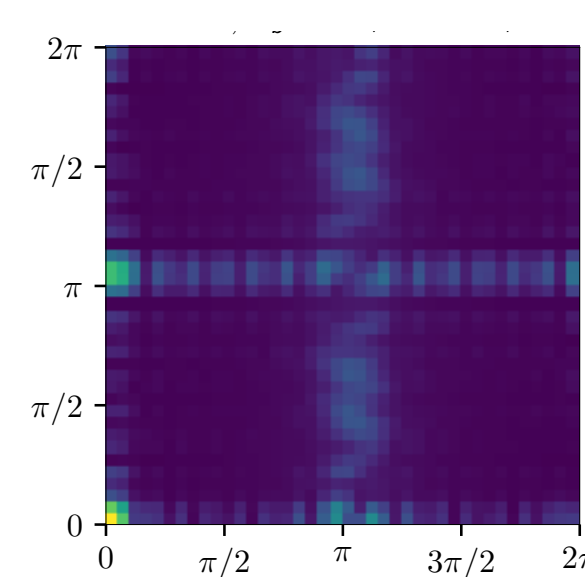
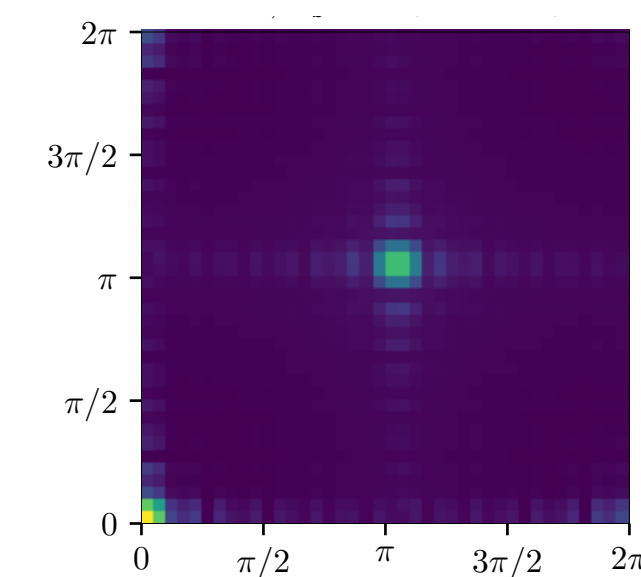
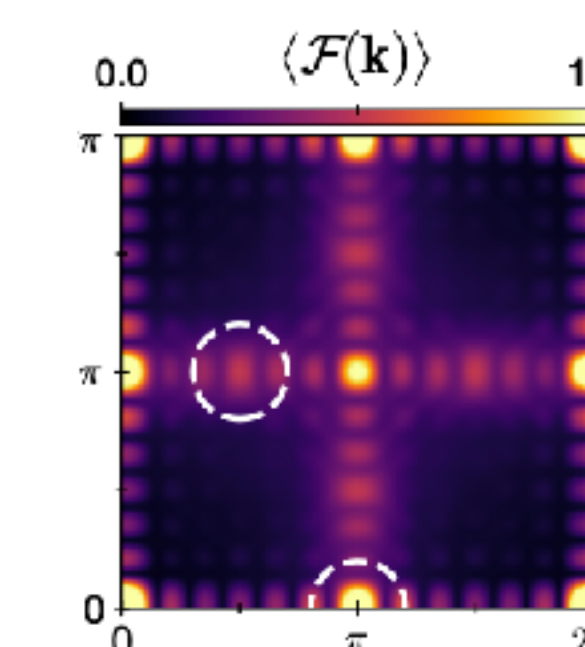
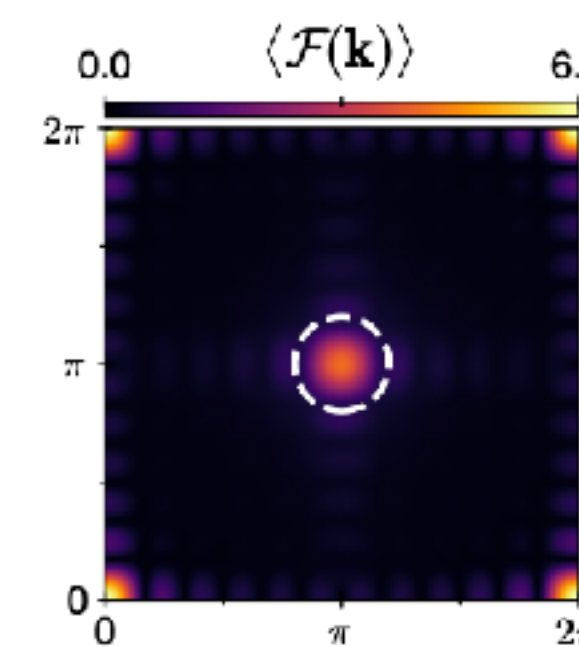
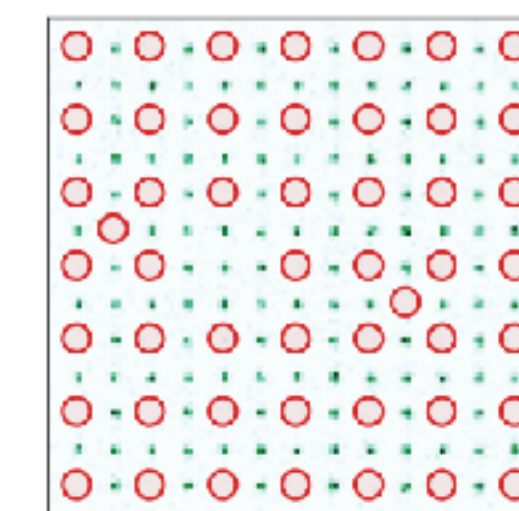
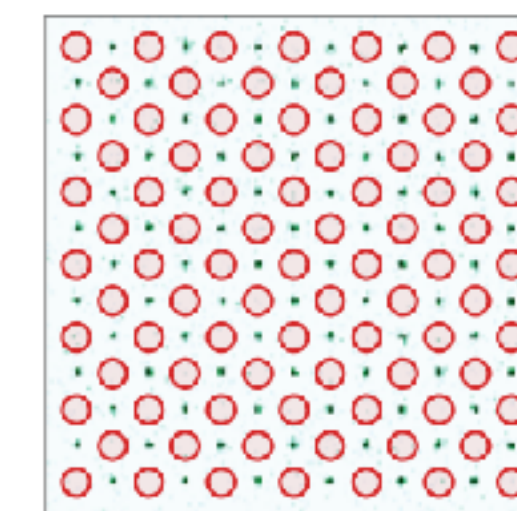
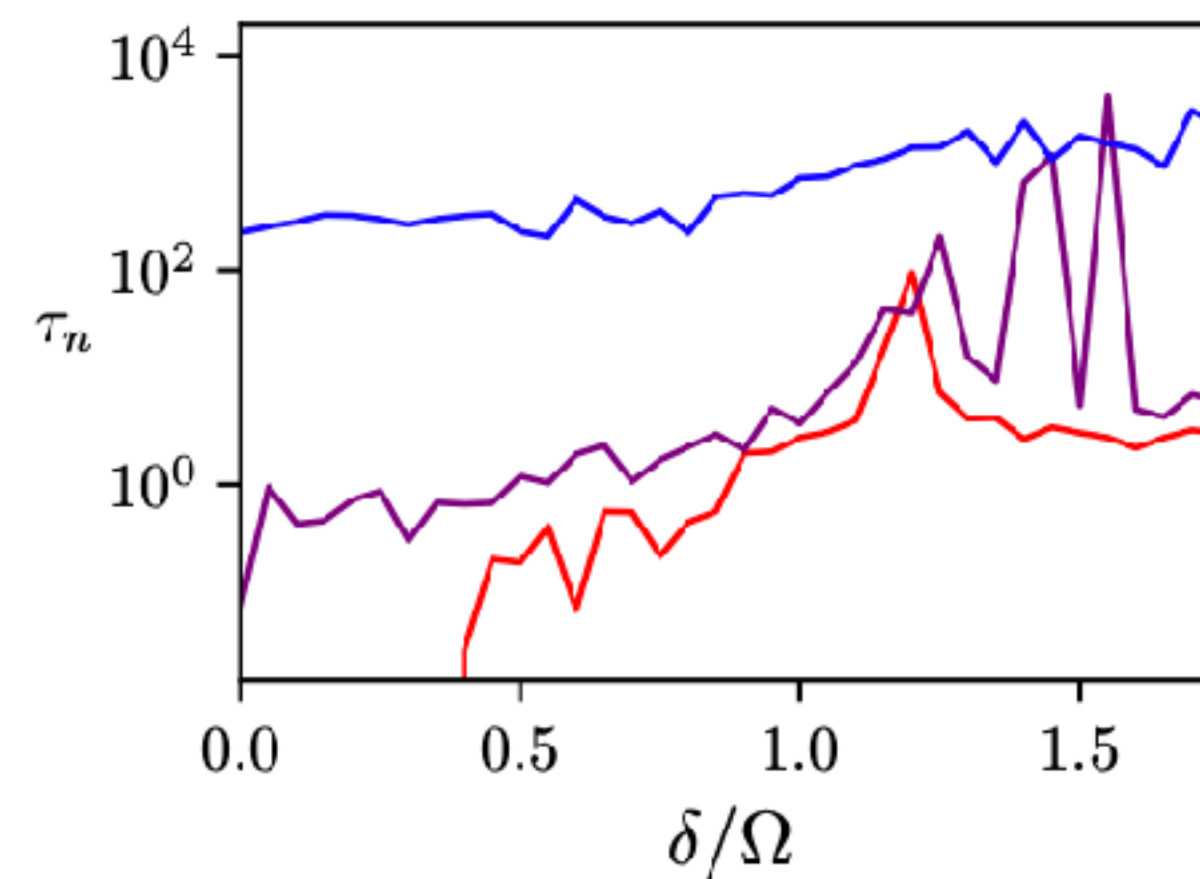
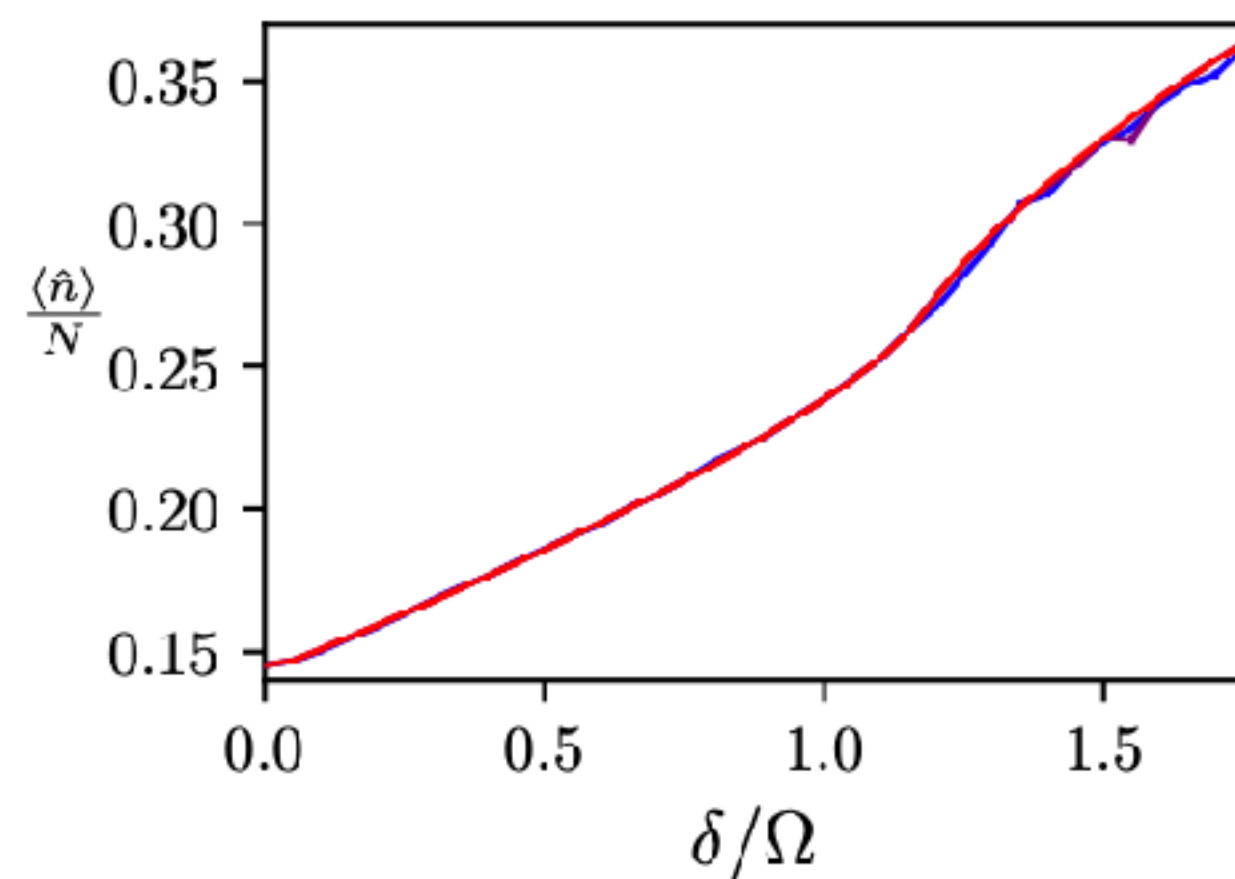
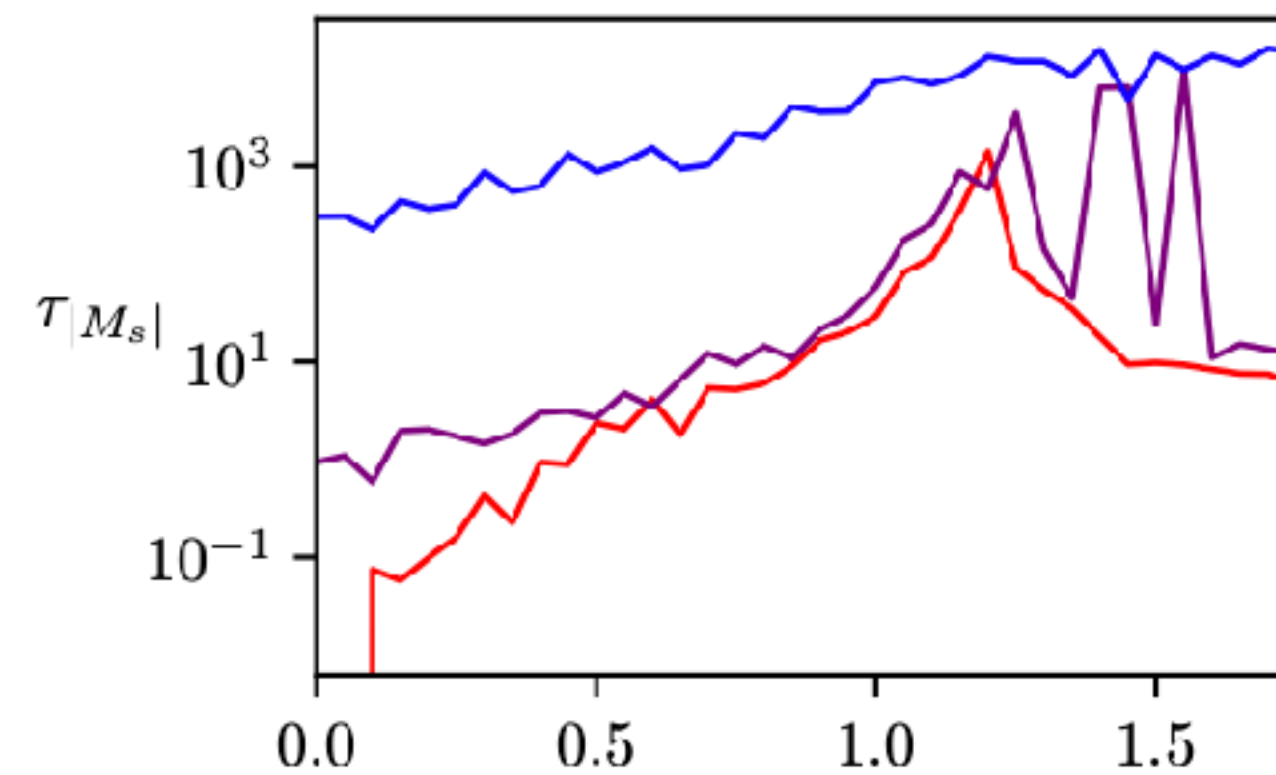
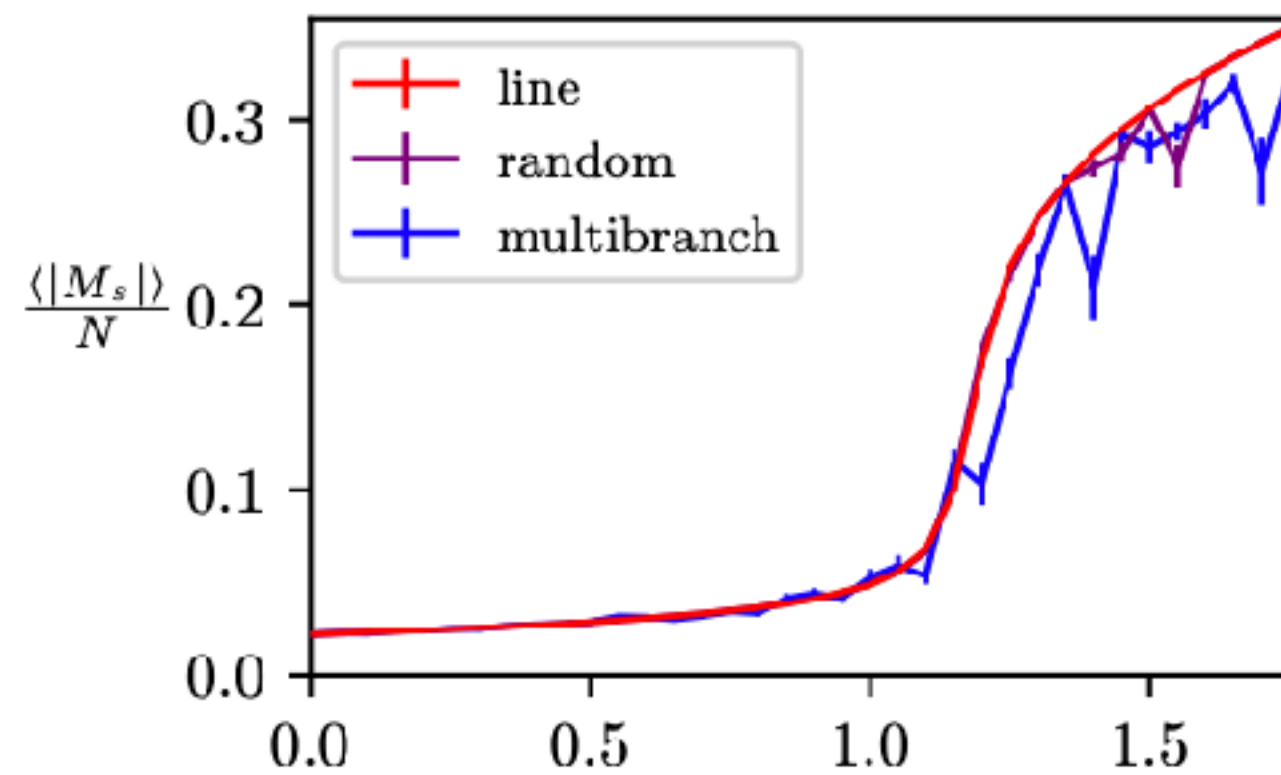
$$\delta_b = \delta / (N - 1)$$

$$C_{ij} = |\min(0, \delta_b, 2\delta_b - V_{ij})|$$

$$Z \equiv \langle \psi_0 | \psi_0 \rangle = \langle \alpha_l | (-\hat{H})^M (-\hat{H})^M | \alpha_r \rangle$$



Efficient QMC: sign-free and ergodic



Merali, De Vlugt, RGM, arXiv:2107.00766
S. Czischek *et al.*

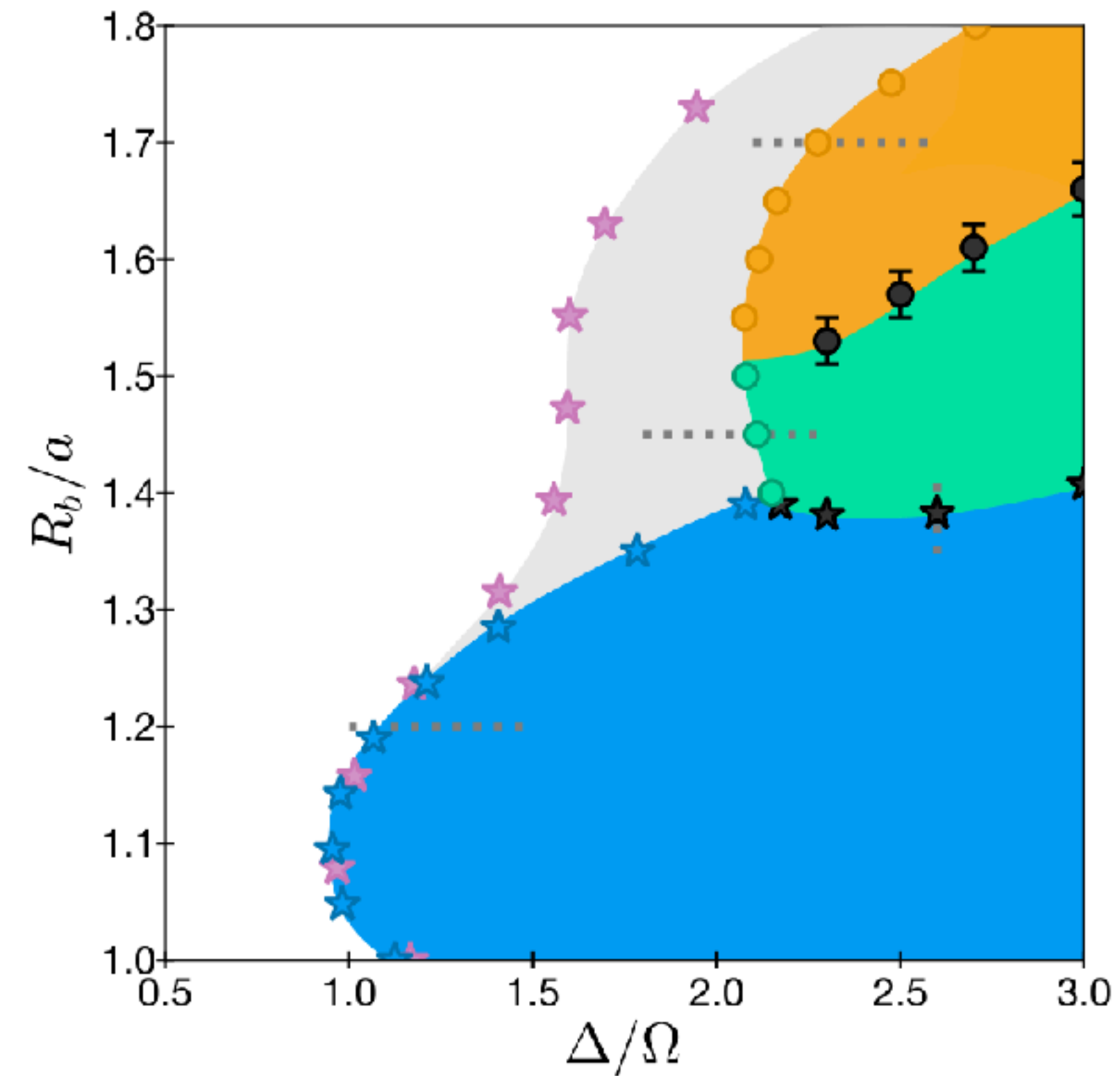
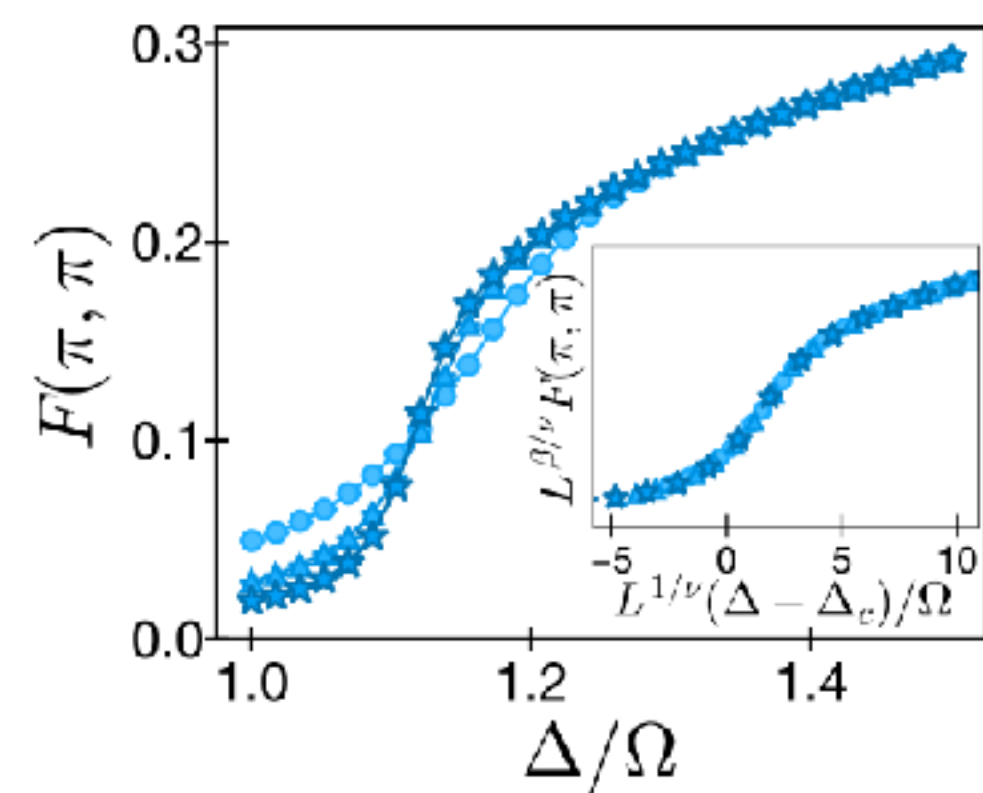
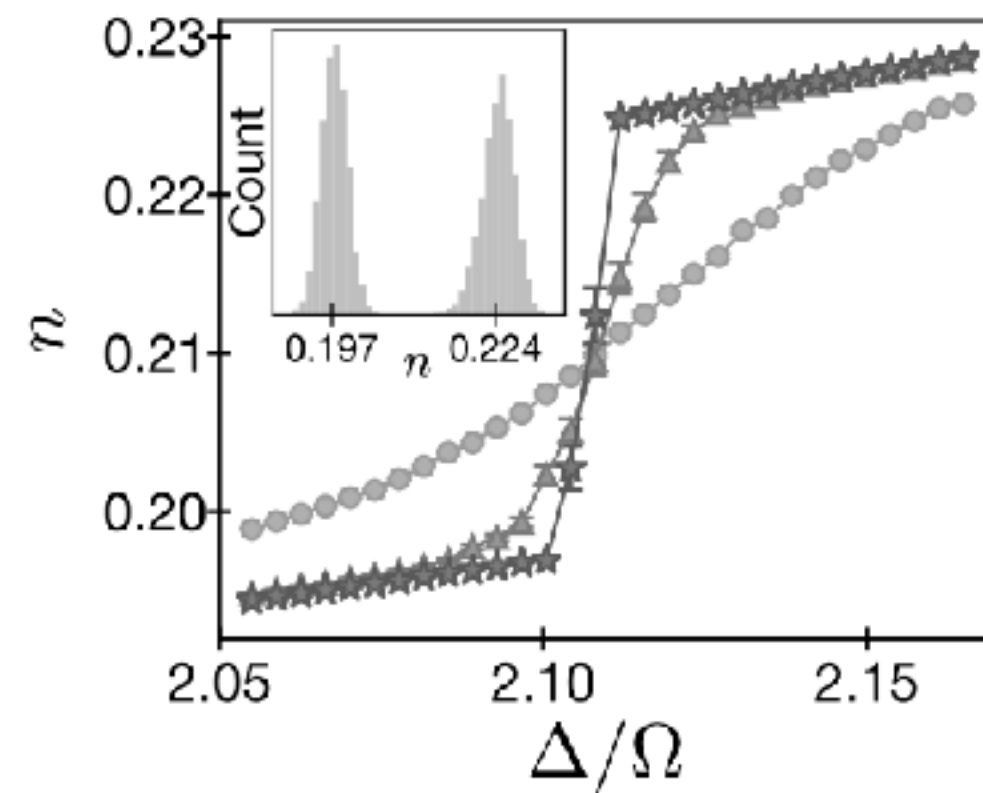
- Detailed comparisons with experiment are possible
- Autocorrelation times can be very significant
- Not clear what the maximum lattice sizes are at this time

Continuous imaginary time QMC



Bulk and Boundary Quantum Phase Transitions in a Square Rydberg Atom Array
M. Kalinowski, R. Samajdar, RGM, M. Lukin, S. Sachdev, S. Choi, arXiv:2112.10790

$L = 8$
 $L = 12$
 $L = 16$



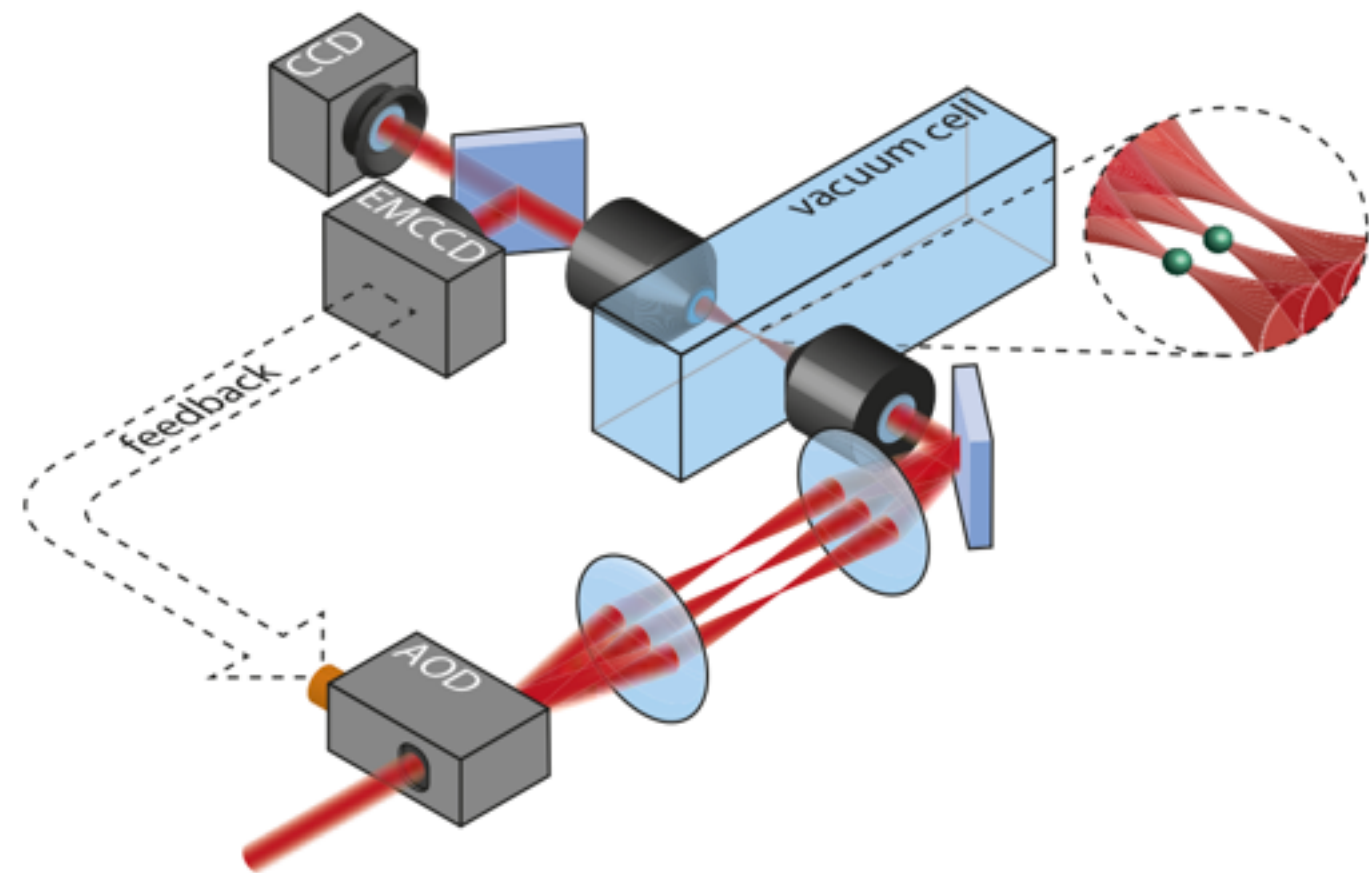
- Clear differences between OBC and PBC systems - boundary plays major role
- Consequences for adiabatic state preparation, optimization problems

Outline

- Rydberg array quantum simulators/emulators
- *In silico* simulation strategies: DMRG, QMC
- Data-driven strategies: neural network wavefunctions & VMC

Data driven state reconstruction

The availability of high quality projective measurement data allows for state reconstruction, e.g. through the KL divergence or maximum likelihood methods



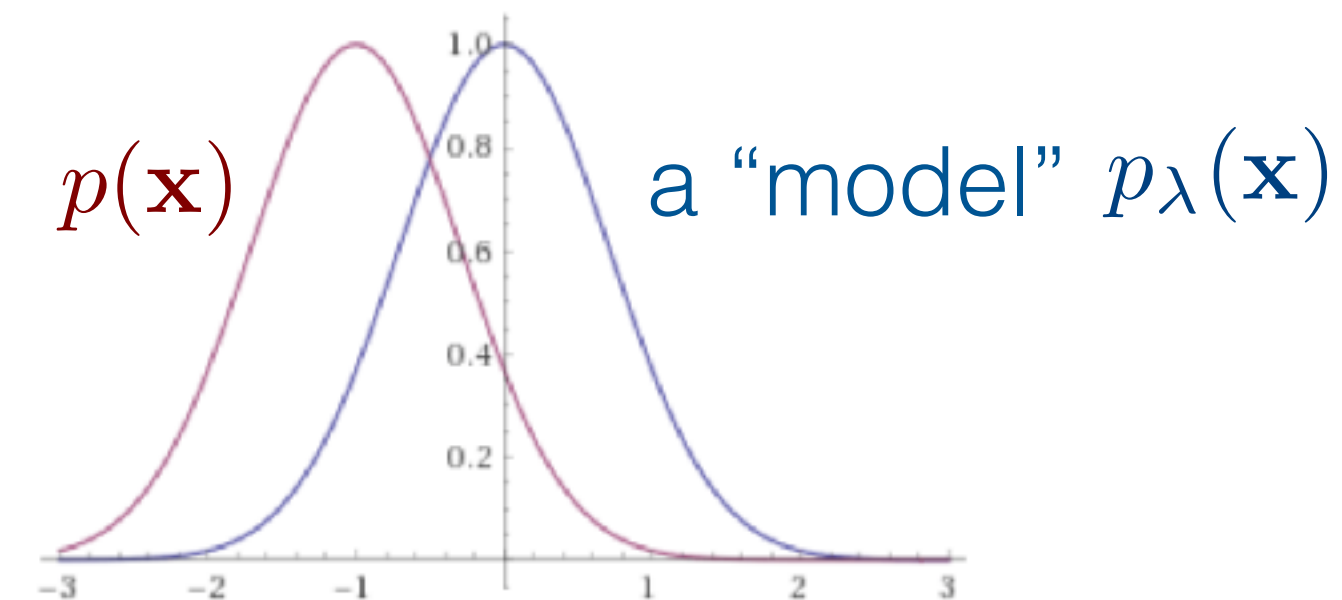
qubit projective measurement data distributed according to Born rule, $p(\mathbf{x})$

$$\begin{aligned} \mathbf{x}_1 &= (1, 0, 0, 1, 1, 1, 0, 0, 0, 0, \dots, 1) \\ \mathbf{x}_2 &= (1, 1, 1, 0, 1, 1, 0, 1, 1, 1, \dots, 1) \\ \mathbf{x}_3 &= (0, 1, 1, 0, 0, 1, 0, 1, 0, 1, \dots, 0) \\ &\vdots \end{aligned}$$

} \mathcal{D}

Cost function:

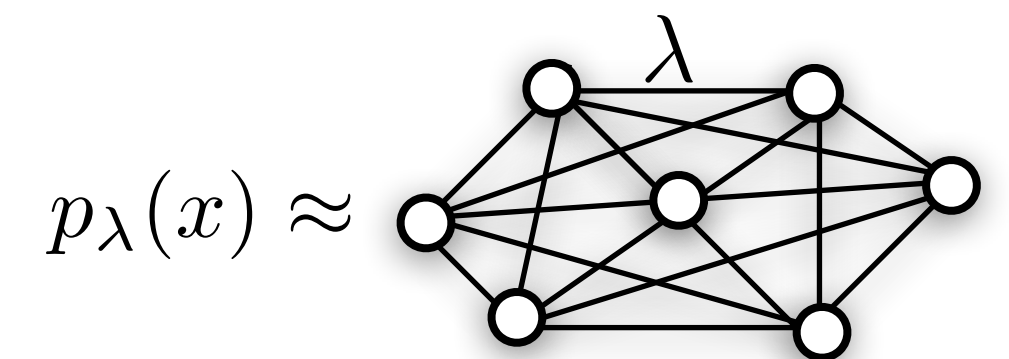
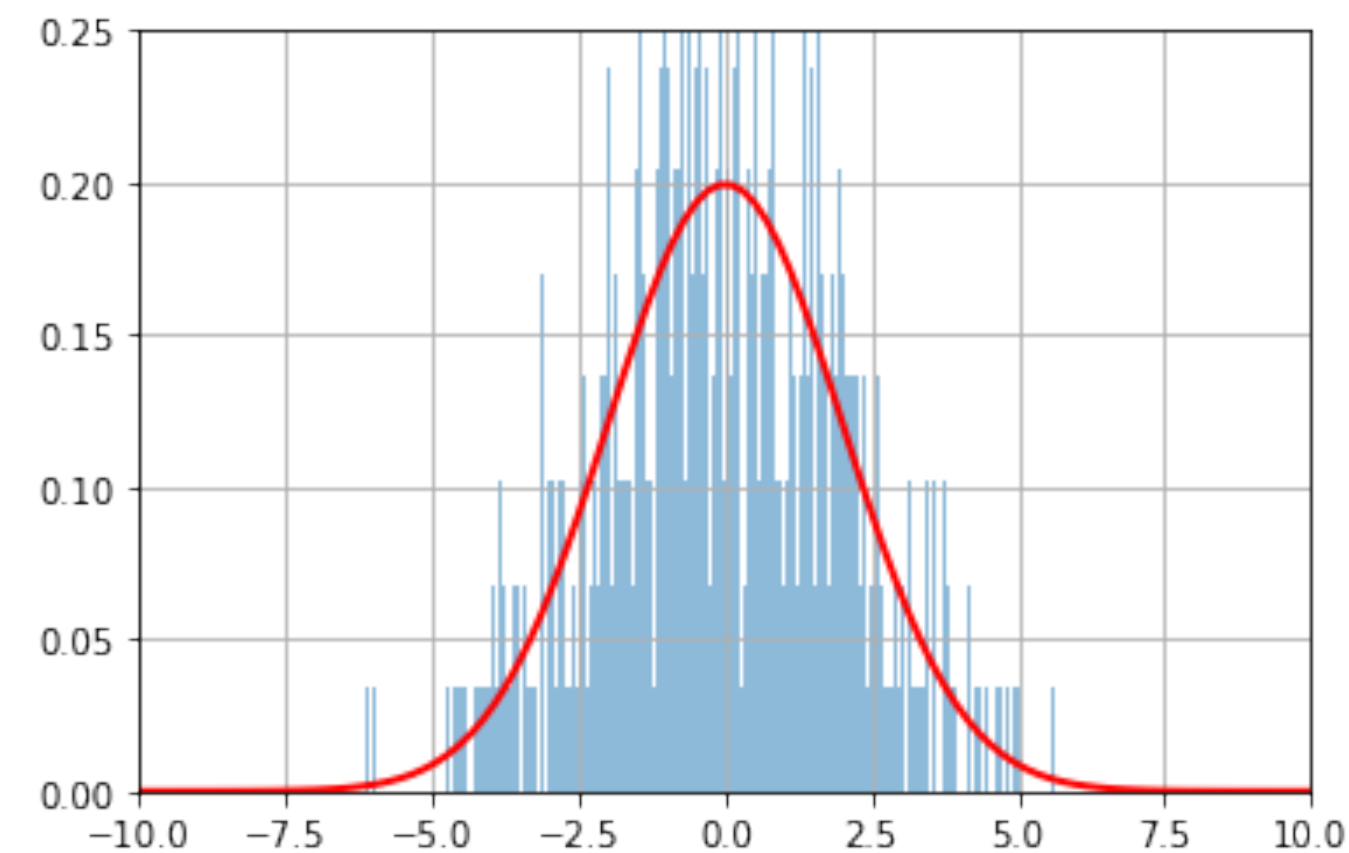
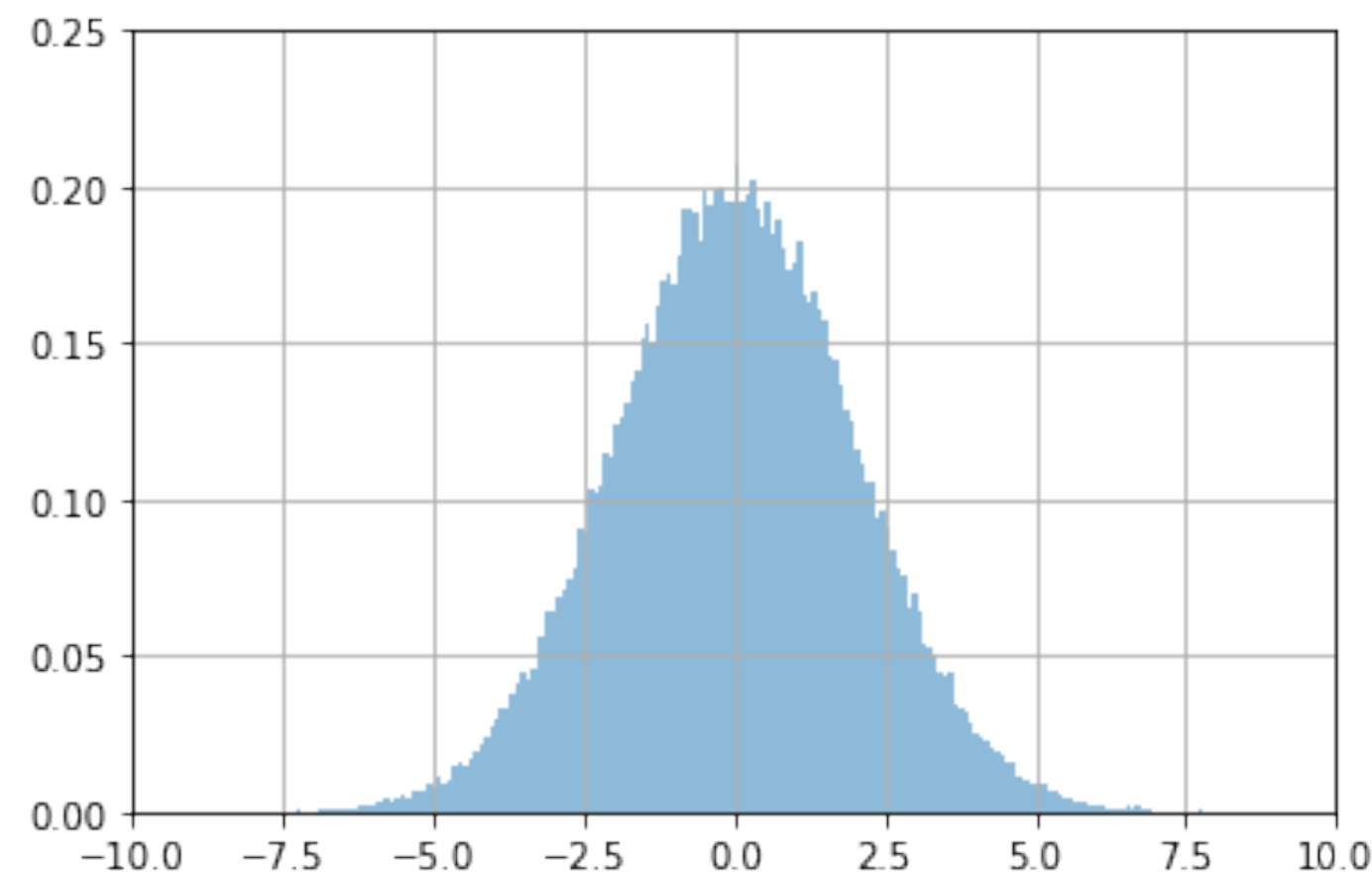
$$\text{KL}(p||p_\lambda) = \sum_{\mathbf{x}} p(\mathbf{x}) \log \frac{p(\mathbf{x})}{p_\lambda(\mathbf{x})} \geq 0$$



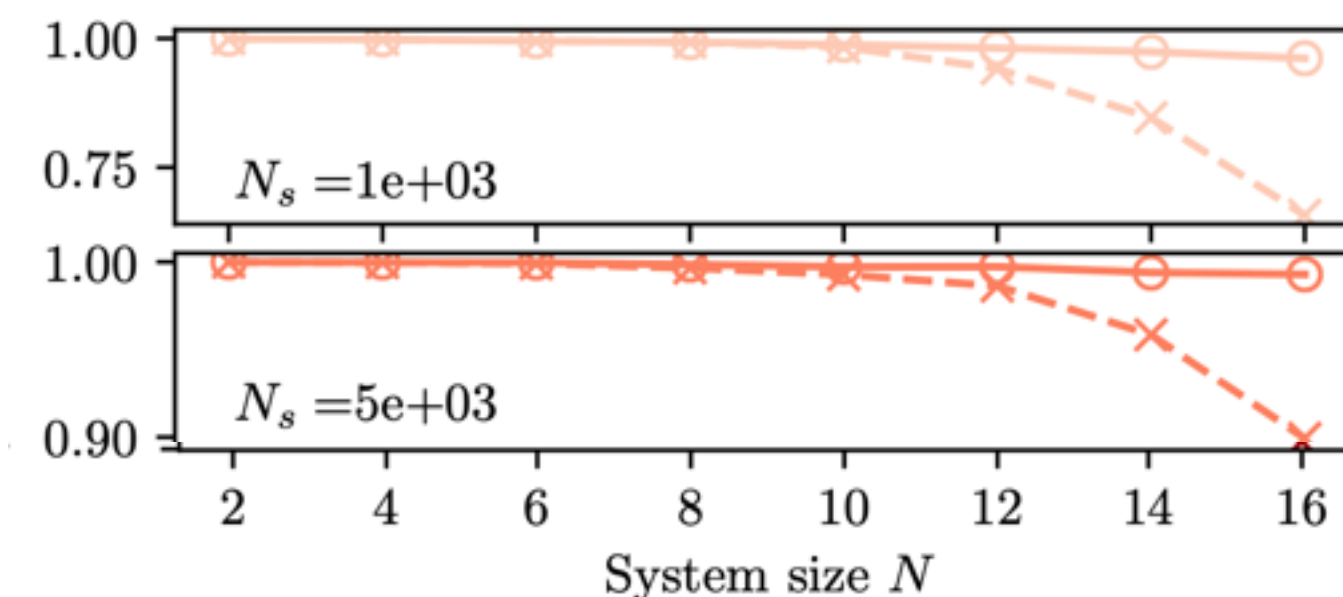
Parameterized models and generalization

- Rydberg data is limited by the experimental shot budget ($\sim 3/s$)
- *Generative models* use inductive bias (assumptions in the model) in order to help generalize to unseen data

$$p(x) \approx \frac{1}{\|\mathcal{D}\|} \sum_{\mathbf{x}_k \in \mathcal{D}} \delta_{\mathbf{x}, \mathbf{x}_k}$$



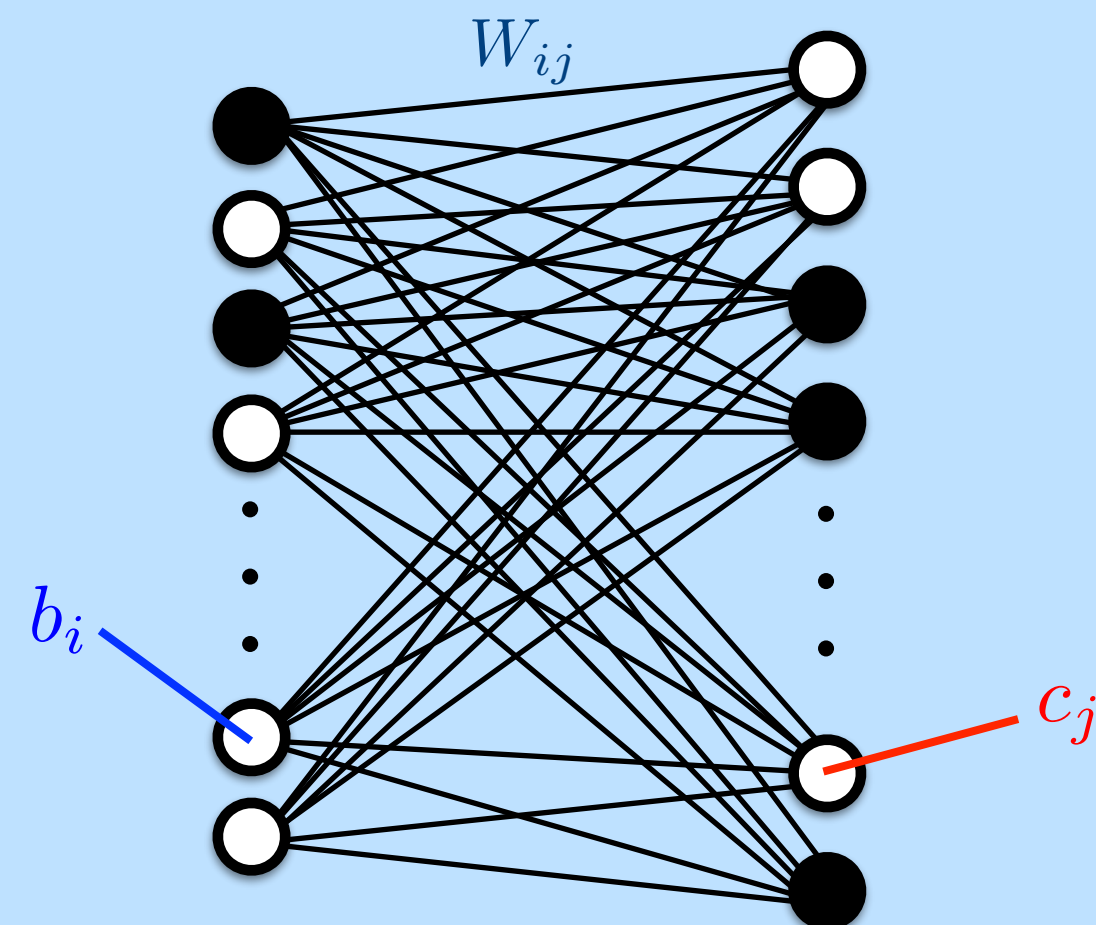
Fidelity improvements for RBMs vs. frequency-distribution reconstructions, for a selection of dataset sizes N_s .



Neural network wavefunctions

Torlai and RGM, Phys. Rev. B 94, 165134 (2016); Carleo, Troyer Science 355, 602 (2017)
 Hibat-Allah, Ganahl, Hayward, RGM, and Carrasquilla, Phys. Rev. Research 2, 023358 (2020)

Restricted Boltzmann Machine



$$p_\lambda = \frac{1}{Z_\lambda} e^{-E_\lambda(\mathbf{x}, \mathbf{h})}$$

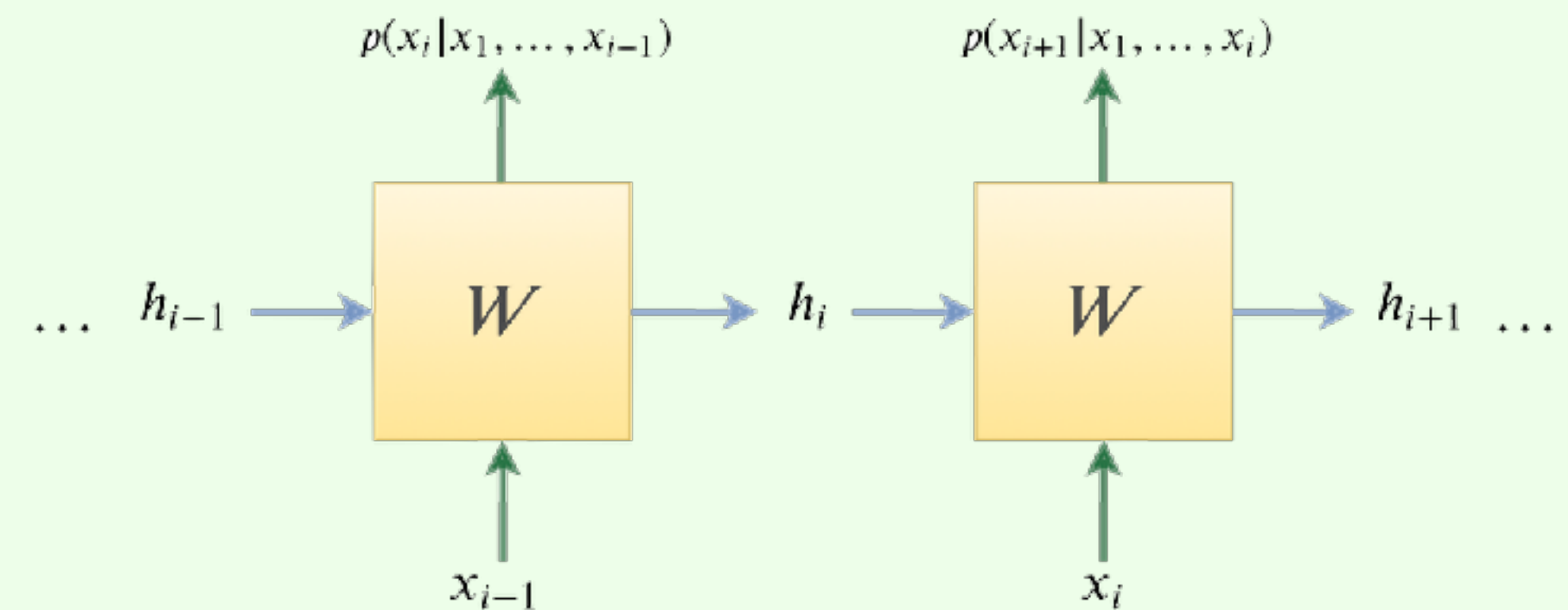
$$p_\lambda(\mathbf{x}) = \sum_{\mathbf{h}} p_\lambda(\mathbf{x}, \mathbf{h})$$

$$x_i = 0, 1 \quad h_j = 0, 1$$

$$E_\lambda(\mathbf{x}, \mathbf{h}) = - \sum_{ij} W_{ij} x_i h_j - \sum_i b_i x_i - \sum_j c_j h_j$$

$$\lambda = \{W, b, c\} \text{ model parameters}$$

Recurrent Neural Network



$$p_\lambda(x_1, \dots, x_N) = \prod_{i=1}^N p(x_i | x_1, \dots, x_{i-1})$$

$$= p(x_1) p(x_2 | x_1) p(x_3 | x_1, x_2) \dots$$

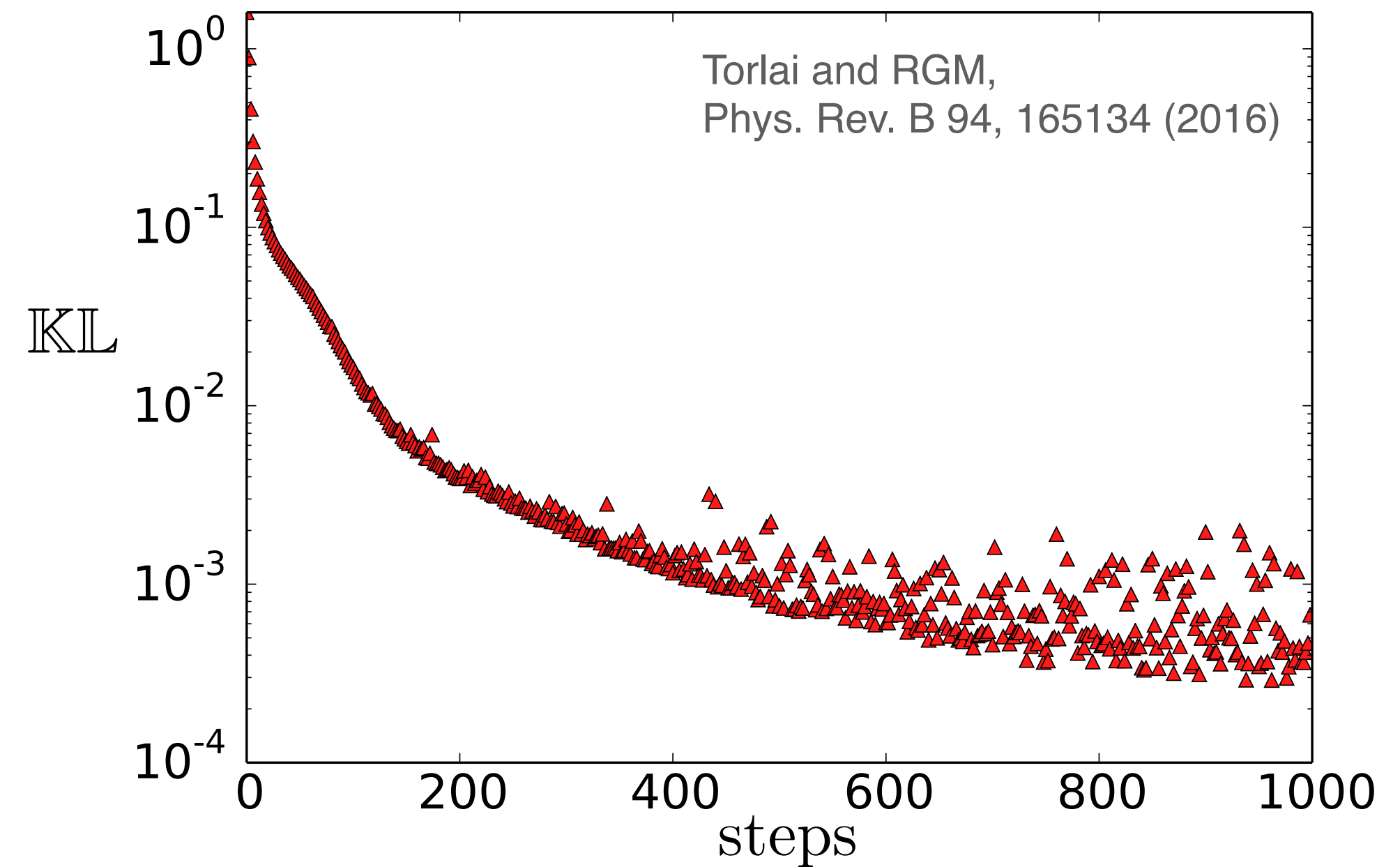
Autoregressive model; produces independent samples

Training & sampling

Training: stochastic gradient descent:

$$\lambda' = \lambda - \eta \nabla \text{KL}$$

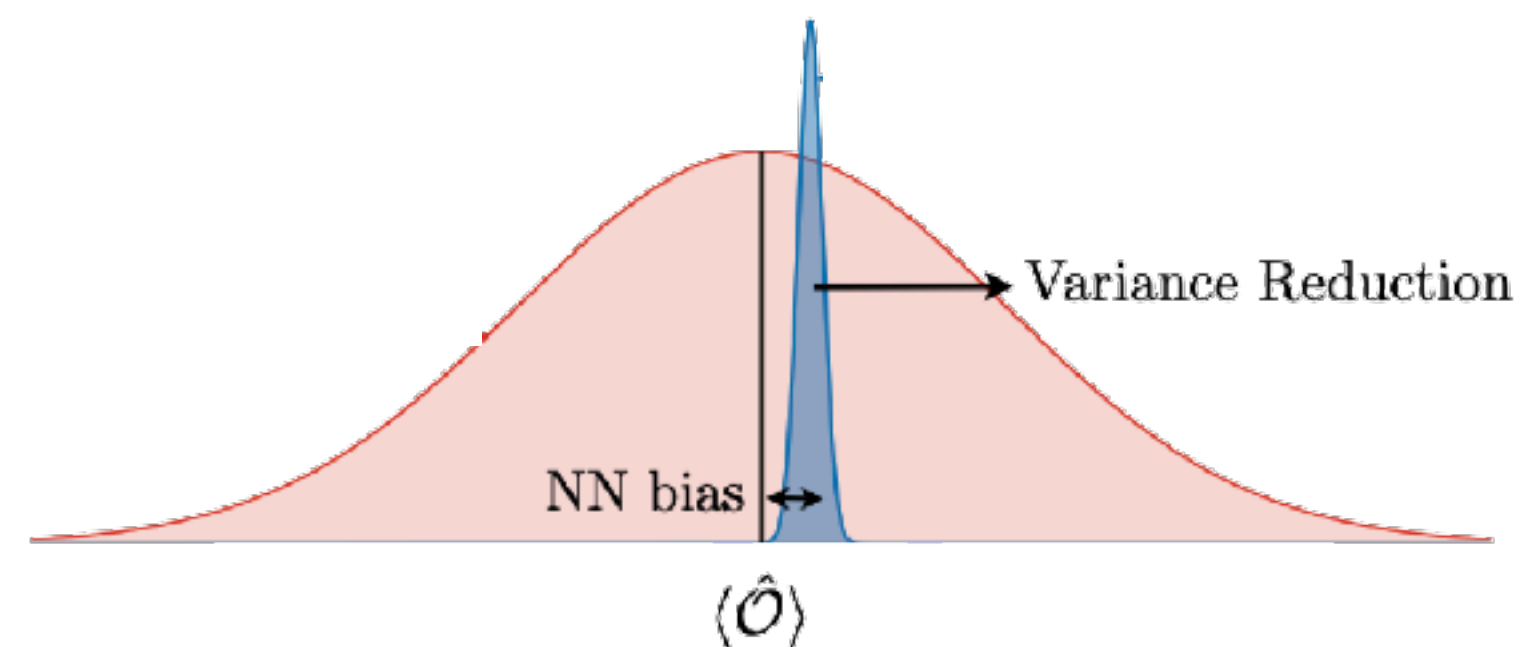
$$\text{KL}(p||p_\lambda) = \sum_{\mathbf{x}} p(\mathbf{x}) \log \frac{p(\mathbf{x})}{p_\lambda(\mathbf{x})} \geq 0 \quad \mathcal{L} = \langle \log p_\lambda(\mathbf{x}) \rangle_p$$



Rydberg Hamiltonian: occupation basis is informationally complete $\psi_\lambda(\mathbf{x}) = \sqrt{p_\lambda(\mathbf{x})}$

Can reconstruct estimators by sampling the trained model

$$\langle A^D \rangle = \sum_{\mathbf{x}} p_\lambda(\mathbf{x}) A_{\mathbf{x}}$$



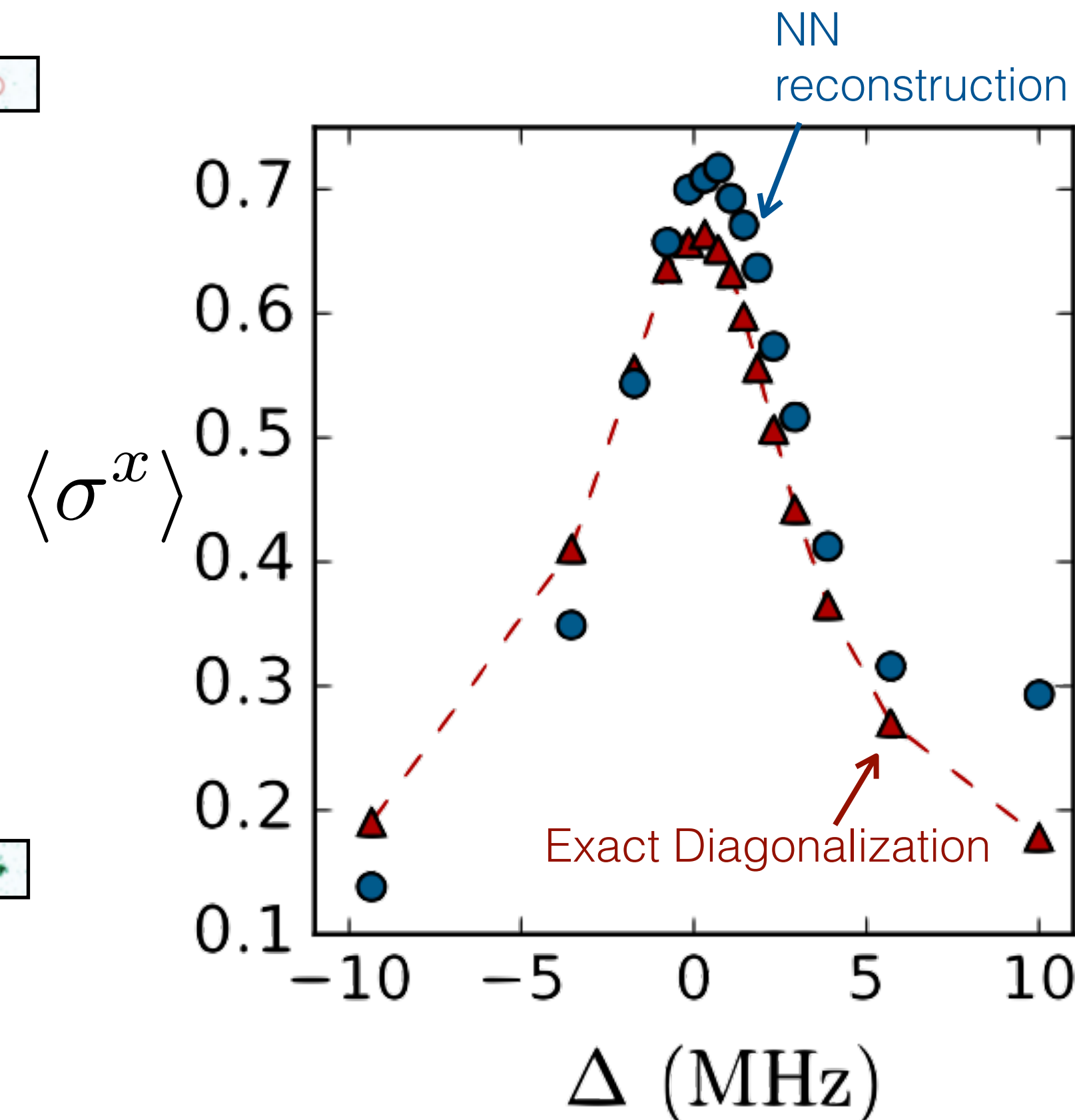
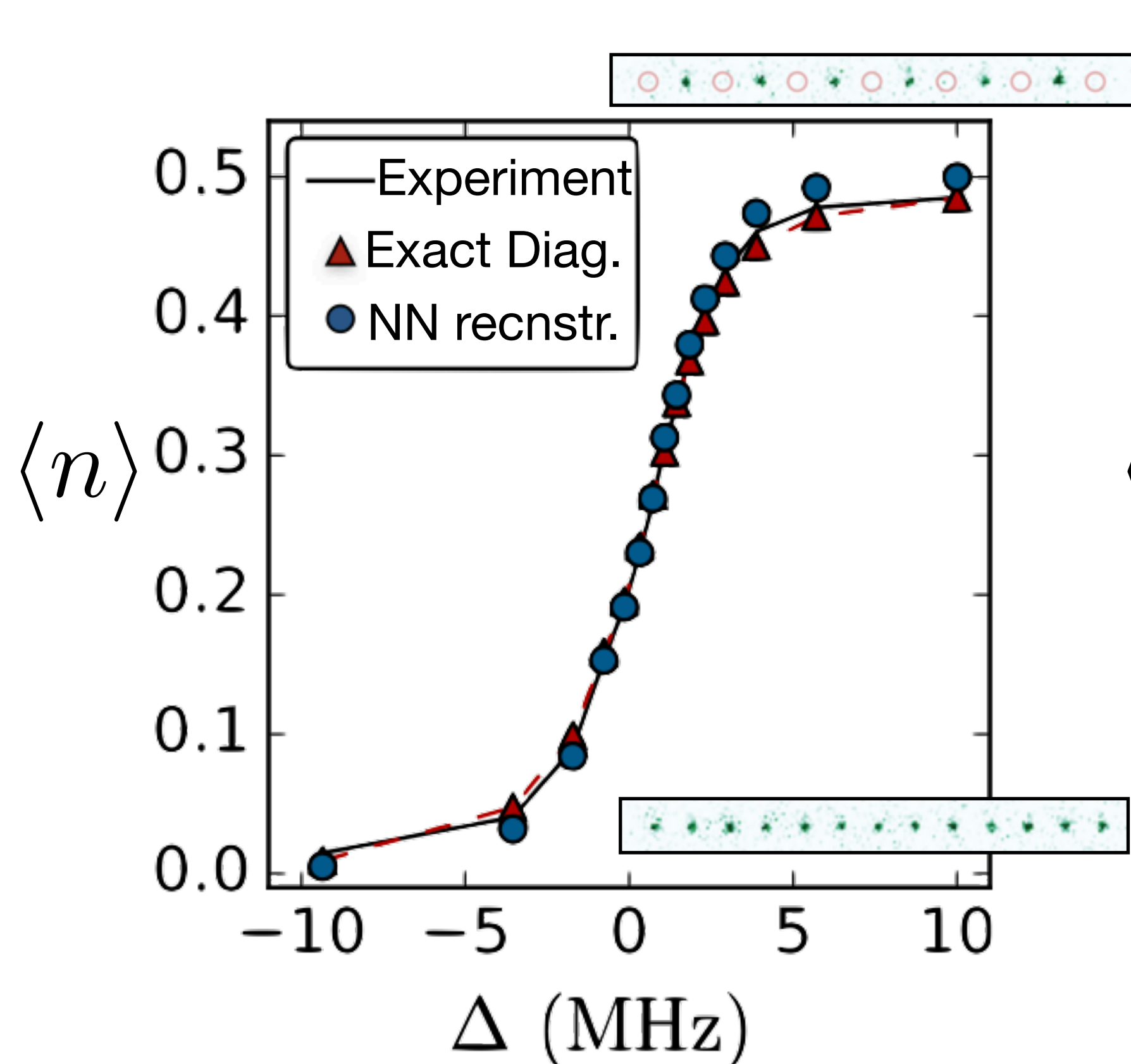
Bias-variance tradeoff

Torlai, Mazzola, Carleo, and Mezzacapo Phys. Rev. Research 2, 022060 (2020)

Rydberg state reconstruction

Torlai, Timar, van Nieuwenburg, Levine, Omran, Keesling, Bernien, Greiner, Vuletić, Lukin, RGM, Endres, Phys. Rev. Lett. 123, 230504 (2019)

- one-dimensional chain
- 3000 projective measurements per detuning parameter
- assume positivity & purity of the state - use RBM



Stoquastic Hamiltonian:

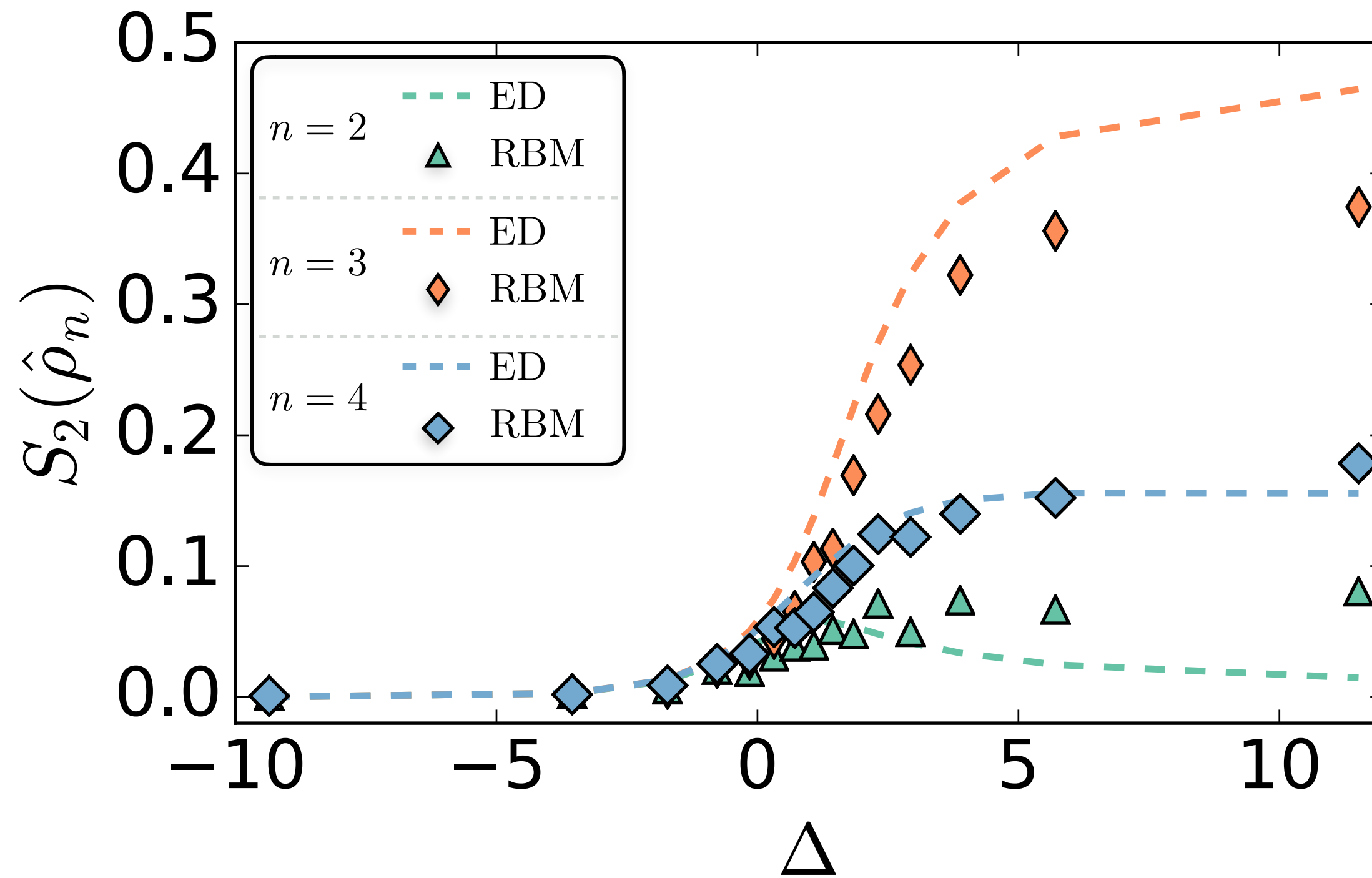
$$\psi_\lambda(z) = \sqrt{p_\lambda(z)}$$

$$\langle \mathcal{O} \rangle = \sum_{zz'} \psi_\lambda(z) \psi_\lambda(z') \mathcal{O}_{zz'}$$

$$= \sum_z \psi_\lambda^2(z) \sum_{z'} \frac{\psi_\lambda(z')}{\psi_\lambda(z)} \mathcal{O}_{zz'}$$

"local" estimator

Experimental reconstruction



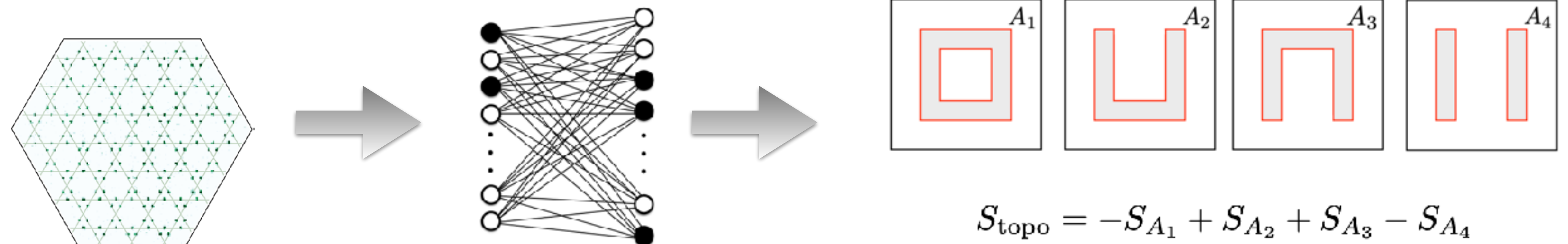
- Second Renyi entropy via SWAP

$$S_2(\rho_A) = -\log [\text{Tr}(\rho_A^2)]$$

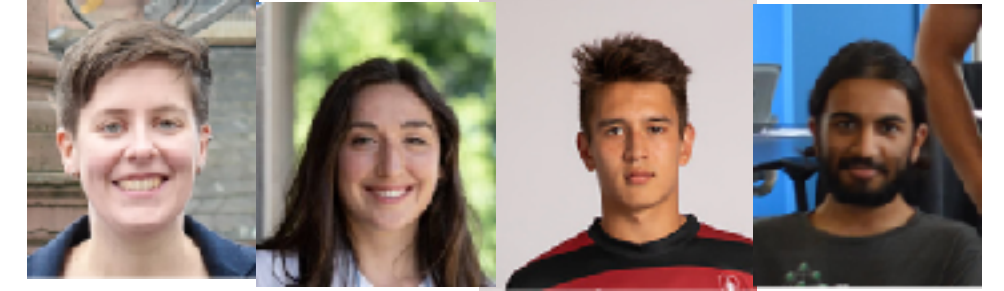
$$\text{Tr}(\rho_A^2) \Leftrightarrow \text{Diagram with two pairs of nodes and four loops (two red, two blue)}$$

$$\text{Diagram with two pairs of nodes and two crossing lines (one red, one blue)} \Leftrightarrow \langle \text{Swap}_B \rangle$$

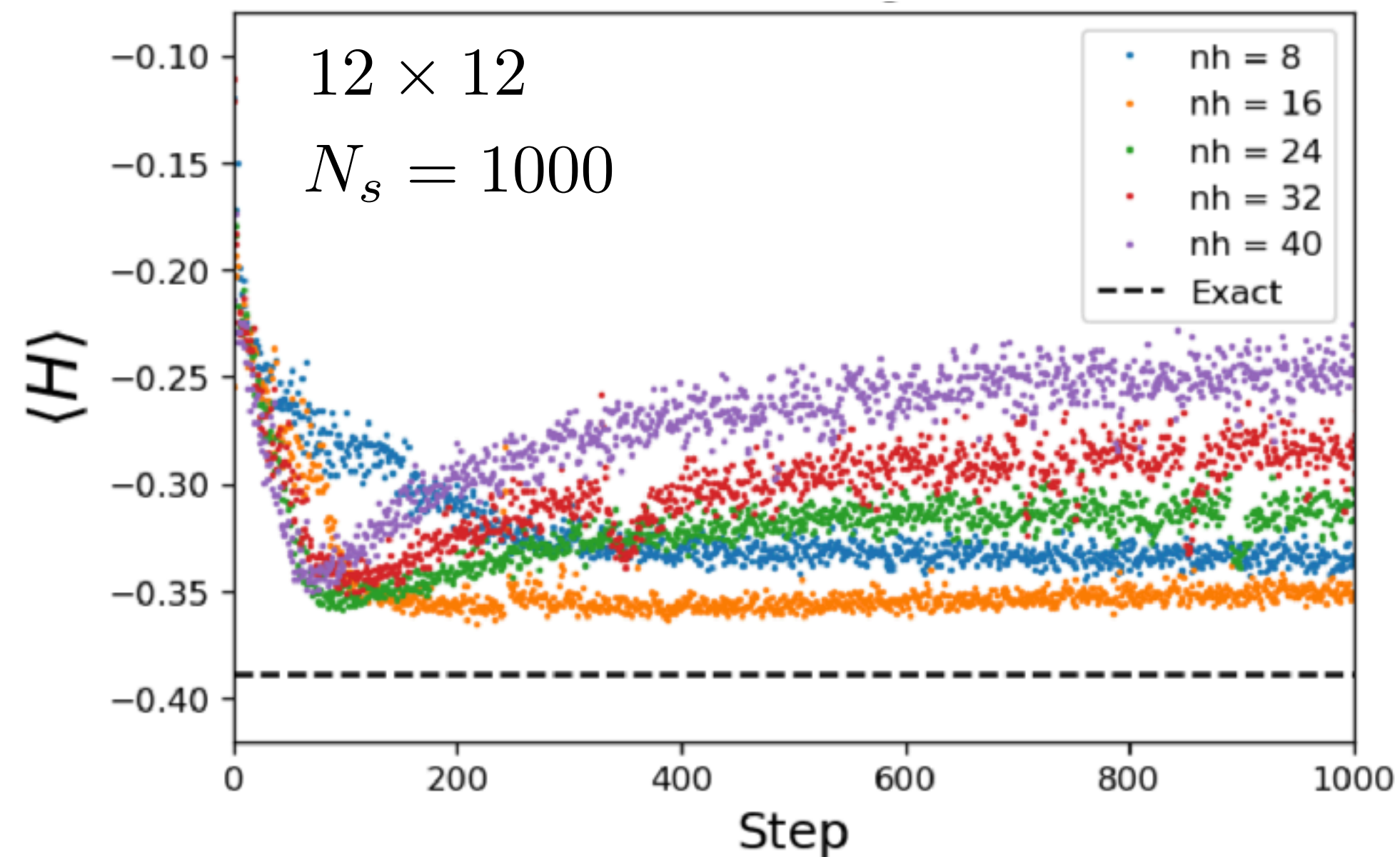
- With more data...



What use is limited experimental data?

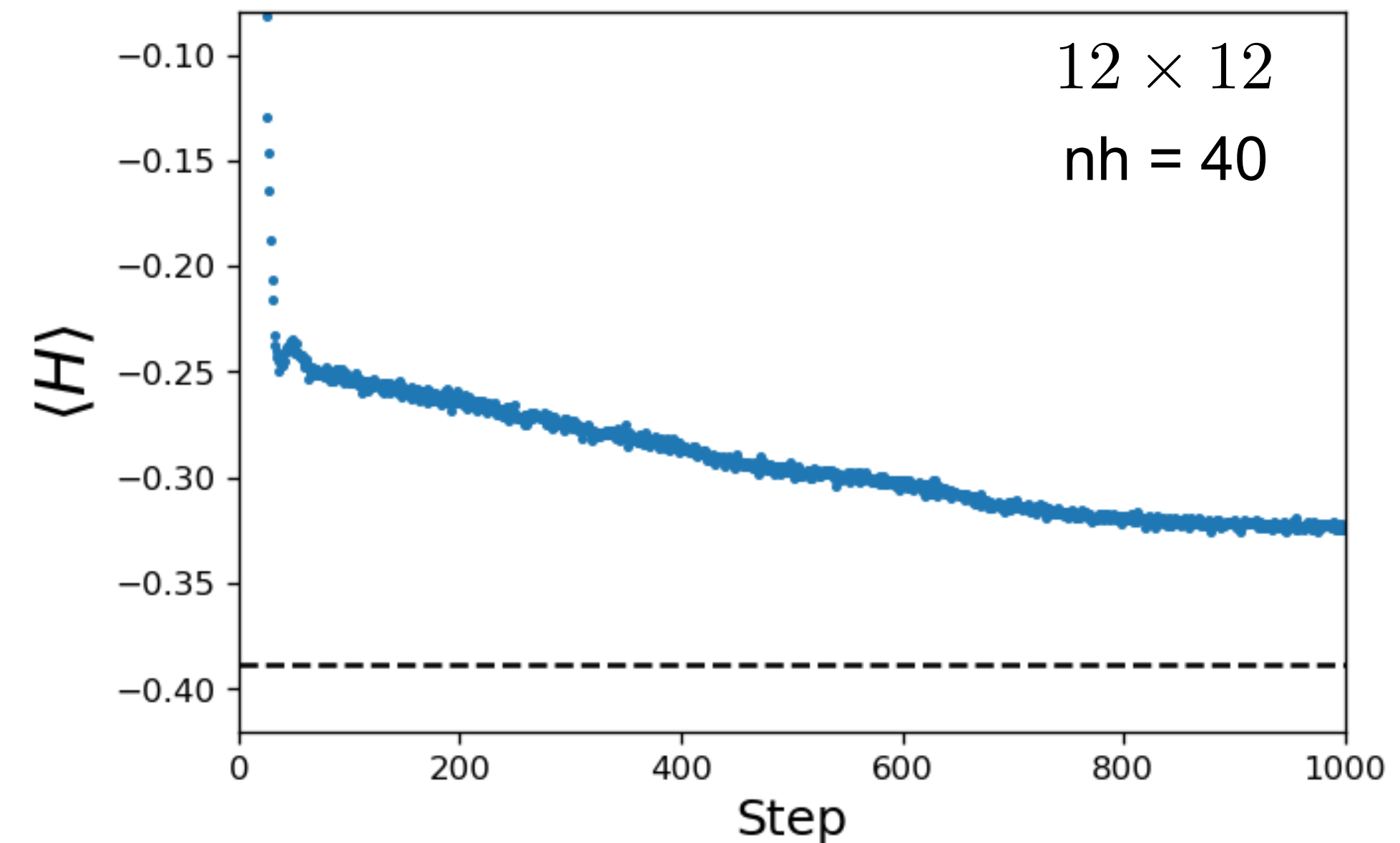


Neural network wavefunctions allow for model parameter optimization in two ways:



Data-driven, e.g. with the K-L divergence

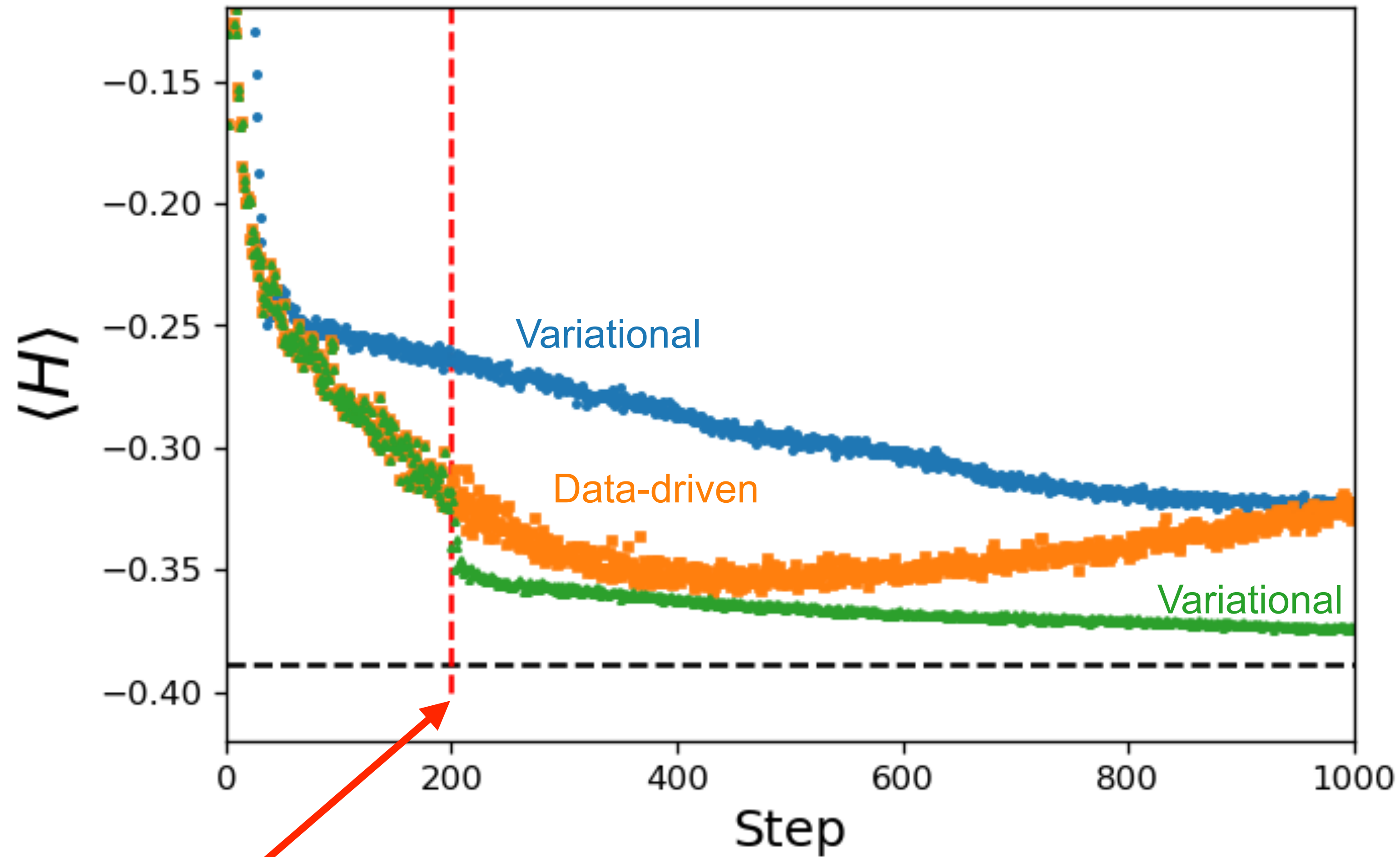
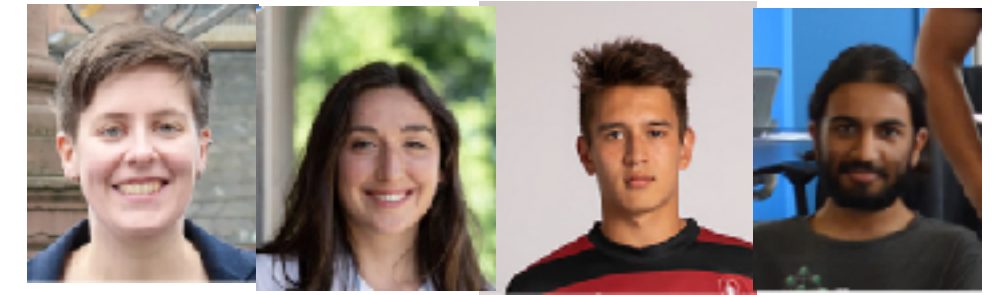
$$\text{KL}(p||p_\lambda) = \sum_{\mathbf{x}} p(\mathbf{x}) \log \frac{p(\mathbf{x})}{p_\lambda(\mathbf{x})} \geq 0$$



Variationally (with knowledge of the Hamiltonian)

$$\langle \psi_\lambda | H | \psi_\lambda \rangle$$

What use is limited experimental data?



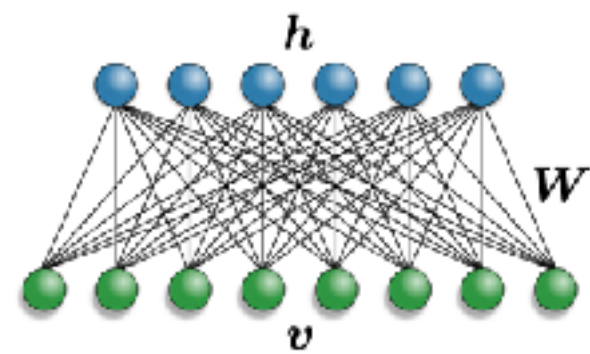
Keep parameters, switch cost functions

Complex quantum states

Torlai, Mazzola, Carrasquilla, Troyer, RGM, Carleo, Nature Physics 14, 447 (2018)
 Torlai and RGM, Annual Review of Condensed Matter Physics 11:325-344 (2020)
 RGM, Carleo, Carrasquilla, Cirac, Nature Physics 15, 887 (2019)

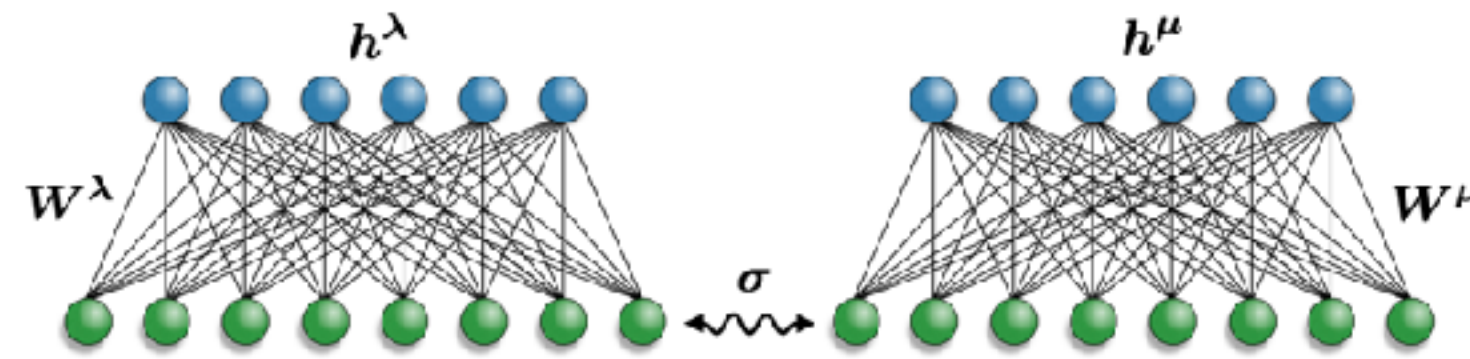
- Conventional generative models can be adapted to learn pure & mixed quantum states

sign free



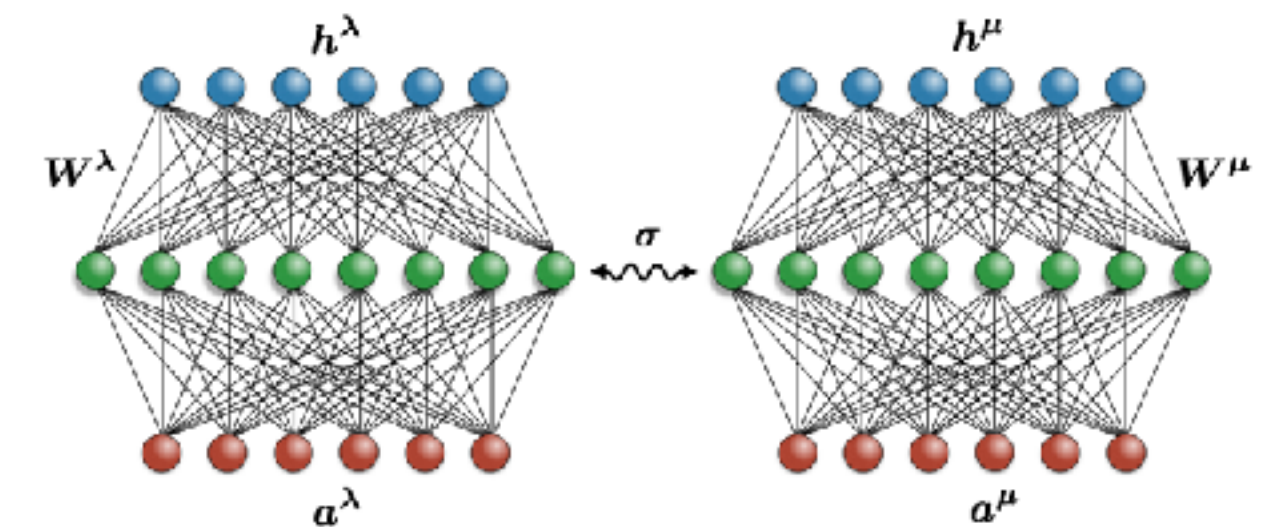
$$\psi_{\lambda}(\mathbf{x}) \propto \sqrt{p_{\lambda}(\mathbf{x})}$$

pure wavefunction



$$\psi_{\lambda,\mu}(\mathbf{x}) \propto \sqrt{p_{\lambda}(\mathbf{x})} e^{i\phi_{\mu}(\mathbf{x})}$$

density matrix



$$\psi_{\lambda,\mu}(\mathbf{x}, \mathbf{a}) \propto \sqrt{p_{\lambda}(\mathbf{x}, \mathbf{a})} e^{i\phi_{\mu}(\mathbf{x}, \mathbf{a})}$$

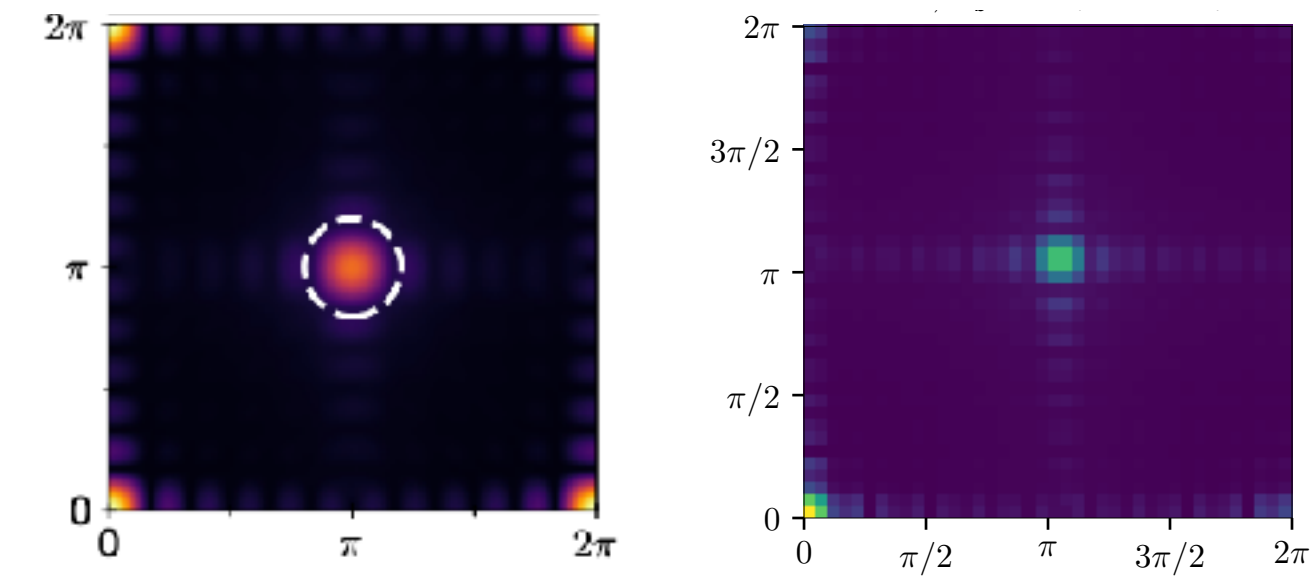
$$\rho_{\lambda,\mu}(\mathbf{x}, \mathbf{x}') = \sum_{\mathbf{a}} \psi_{\lambda,\mu}(\mathbf{x}, \mathbf{a}) \psi_{\lambda,\mu}^*(\mathbf{x}', \mathbf{a})$$

- Will make the data driven problem that much harder

$$\mathcal{L} = \sum_b \sum_{\mathbf{x}_b} \log |\psi_{\lambda,\mu}(\mathbf{x}_b)|^2$$

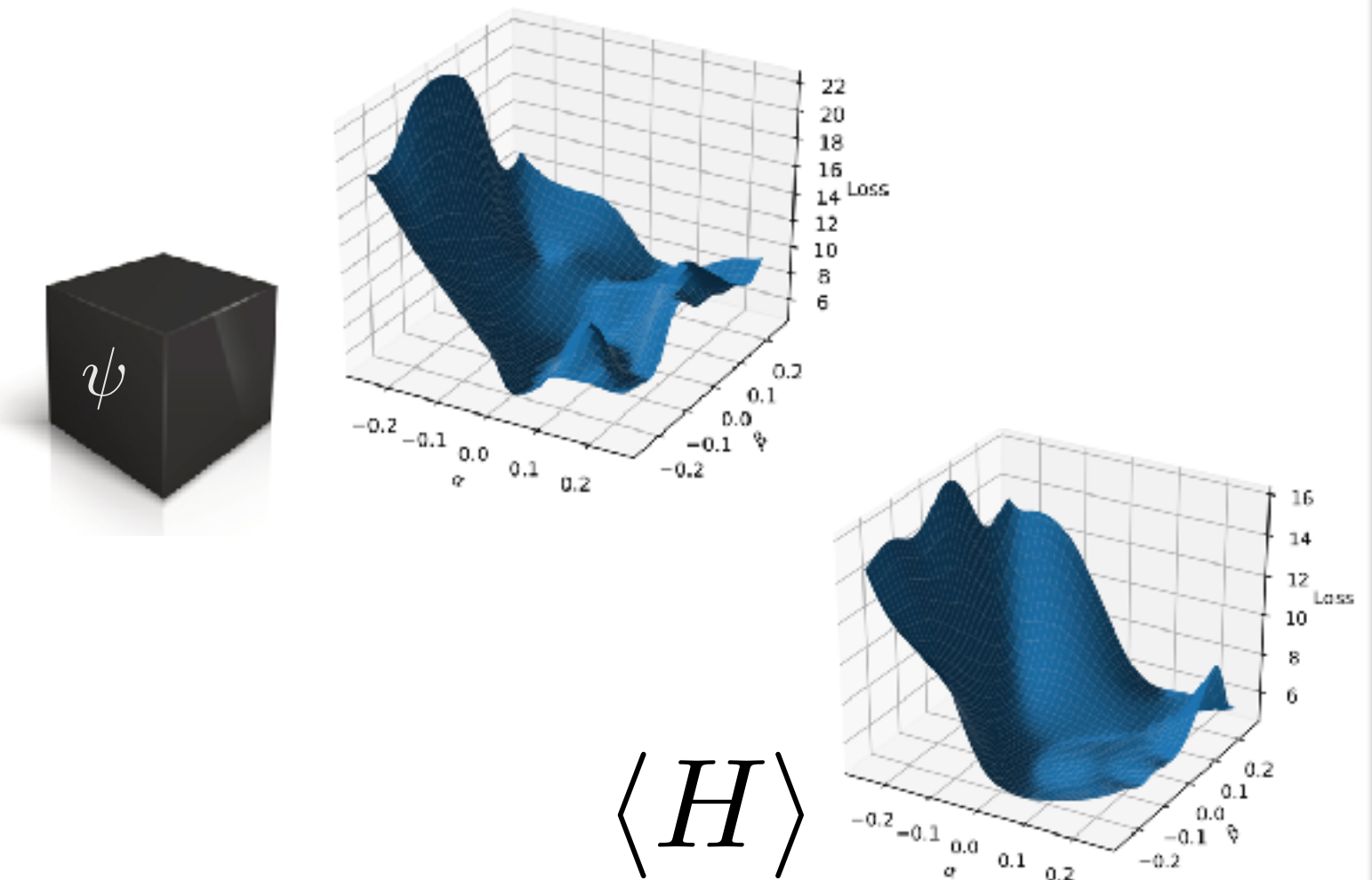
Discussion: Rydberg atom arrays

- A platform for exciting physics



- Classical simulations can reproduce current experiments - but for how long?

- Projective (experimental) measurement data opens up the possibility of combining *data-driven* with *variational* parameter learning.



- Experiments are capable of producing other Hamiltonians, including non-stoquastic models (eg. XXZ)

$$H = \sum_{i \neq j} J_{ij} \sigma_i^z \sigma_j^z + J'_{ij} (\sigma_i^x \sigma_j^x + \sigma_i^y \sigma_j^y)$$

Scholl *et al.*, arXiv:2107.14459